



THERMOELASTIC PROPERTIES IN COMBINED BENDING AND EXTENSION OF THIN COMPOSITE LAMINATES WITH TRANSVERSE MATRIX CRACKS

ERIK ADOLFSSON and PETER GUDMUNDSON

Department of Solid Mechanics, Royal Institute of Technology, S-100 44 Stockholm, Sweden

(Received 14 December 1995; in revised form 15 July 1996)

Abstract—Approximate analytic expressions for the thermoelastic properties in combined bending and extension of composite laminates containing transverse matrix cracks are derived. The model covers two-dimensional laminates of arbitrary lay-up sequences. The derived expressions for the compliances and thermal expansion coefficients merely contain ply property data and crack distributions. In order to check the accuracy and reliability of the presented analytic method, some sample cracked geometries were examined by use of the finite element method. A good agreement was found between the numerically and analytically obtained results for all cases under consideration.
© 1997 Elsevier Science Ltd.

1. INTRODUCTION

Since advanced fibre reinforced composites were made commercially available, considerable attention has been devoted to the analysis of the characteristic mechanical properties of these materials. The obvious benefits attached to the use of continuous fibre reinforced composite laminates, e.g. the possibility of *in situ* designing unique material properties, are accompanied by some apparent drawbacks. Damage modes which are not found in homogeneous materials play a principal role for the degradation of compounds of fibres and matrix material. Such distinguishing modes of damage are matrix cracking, fibre failure, fibre-matrix debonding and delamination. Matrix cracking is often the first defect that occurs in a composite laminate subjected to a quasi-static or cyclic tensile load, see Masters (1981), Highsmith and Reifsnider (1982) and Jamison and Reifsnider (1982). The matrix cracks are, however, seldom critical from a structural failure point of view, but in many cases trigger delaminations and fibre fracture, confer Highsmith and Reifsnider (1982). Apart from serving as originators for more severe forms of damage, the matrix cracks will considerably impair the stiffnesses of the laminate. Östlund and Gudmundson (1992) stated on the basis of finite element calculations, that for a $[\pm 55]$ glass fibre reinforced epoxy laminate, matrix crack induced delaminations primarily affect the out-of-plane effective stiffnesses. The major decrease in in-plane stiffnesses originates from the matrix cracks themselves.

The calculation of the stiffness loss in pure extension of composite laminates containing transverse matrix cracks has attracted much attention from the scientific community during the last decades. Aveston and Kelly (1973) along with Hahn and Tsai (1974) were amongst the first researchers to account for a stiffness degradation related to matrix cracks in cross-ply laminates. The methods for prediction of stiffness degradation which have since then emerged from the collected scientific efforts range from the simple ply-discount method adopted by, for example, Sendeckyj *et al.* (1974) to more sophisticated methods using only a minimum of approximations. The ply discount method clearly renders an underestimate of the sought stiffnesses of the cracked laminate, since the load bearing capacity of the damaged plies is assumed to vanish in the direction transverse to the fibres. It is further impossible to include a dependency on the degree of cracking in the separate plies in the ply discount method due to its discrete character. Talreja (1985) pointed out some uncertainties involved with the application of the ply discount scheme, and also stated that

in some cases the overestimations of the reductions in stiffnesses attached to the application of the ply discount method can be very large.

The shear-lag method appropriated by Reifsnider (1977) offers a relatively uncomplicated way of calculating the reduced stiffnesses of cracked laminates. The load transfer between neighbouring plies is assumed to take place in a so-called shear layer of a generally unknown thickness. The shear lag concept in general requires experimental data for its prosperous application. Successful practice of the shear-lag method and its extensions was for cross-ply laminates achieved by, among others, Lim and Hong (1989) and Xu (1995).

Gottesman *et al.* (1980) used expressions for the elastic energy associated with a single crack in an infinite orthotropic sheet to derive expressions for the overall elastic constants of a cracked laminate. The cracks were hence assumed not to interact in this investigation. A more refined analysis within the same frame of reference was undertaken by Gudmundson and Zang (1993). In the latter investigation, crack interaction was taken into account, and the complete tensors of extensional stiffness and thermal expansion for a composite laminate of arbitrary lay-up sequence containing matrix cracks were calculated on closed form.

It can thus be concluded that the problem of reduction in extensional stiffnesses in composite laminates containing matrix cracks has accumulated a thorough treatment in the literature. An extended confirmation of this is given in the review by Abrate (1991). The analyses of the reduction in flexural moduli due to a distribution of transverse cracks are more sparse. In connection with bending, attention has to a larger extent been dedicated to the presence of delaminations. Such investigations have, for example, been undertaken by Tracy and Pardoen (1988) and by Kwon and Weiseman (1991). The former of these two works comprehends three- and four-point bending tests on a beam-like geometry of graphite-epoxy laminates. An analysis based on beam theory as well as finite element results and experimental results are presented. It is seen that the reduction in bending stiffness in three-point bending of a homogeneous beam is as low as 1% for a central through-the-width delamination length of one fourth of the beam length. The decrease in flexural stiffness increases to around 10% if the delamination length reaches half the beam length. For a quasi-isotropic composite laminated beam, on which experiments were carried out, the stiffness reductions were even smaller. The paper by Kwon and Weiseman (1991) shows similar results, but for simply supported square plates of lay-up sequences $[\pm\theta^\circ]$ and $[0^\circ/90^\circ]$ containing a central square delamination. The analyses were performed by use of the finite element method. The reductions in flexural stiffness were around 10% for delaminations covering half the plate size.

The results presented above regarding the reduction of flexural stiffness due to delaminations thus can be regarded in the perspective of those of Östlund and Gudmundson (1992) concerning extensional stiffnesses referred to previously. A large extent of delamination is required before the flexural stiffnesses are affected in any major way. This was also the situation reported on by Östlund and Gudmundson (1992) for the in-plane extensional stiffnesses. Since both the in-plane extensional stiffnesses and the stiffnesses in bending depend strongly on the in-plane stresses in the composite, the results are not surprising. A further comparison implies that the flexural stiffnesses of composite laminates should, to a considerable amount, be affected by transverse matrix cracks. Investigations of the isolated effects of transverse cracking on the bending rigidities of composite laminates are, however, rare in the literature. It should be noted that delaminations and matrix cracks cannot be treated as separate phenomena when coexisting, since strong coupling effects will prevail, see Liu and Malvern (1987) and Liu *et al.* (1993).

Experiments on bi-axial flexural loading of cross-ply carbon fibre reinforced laminated disks performed by Tsangarakis and Taleghani (1995) revealed matrix cracking accompanied by delaminations and fibre fracture. It has been observed by Liu *et al.* (1993), Choi *et al.* (1991a, b), Choi *et al.* (1992) among others, that also when a composite laminate is exposed to impact loads, matrix cracking appears to be the first type of damage to occur, which is then followed by delamination. The effects of low velocity impact on epoxy based composite laminates have by Hong and Liu (1989) been reported similar to those of an applied bending load. The results from the impact tests thus support the hypothesis that matrix cracking is an important incipient damage in bending of composite laminates. The

matrix cracks will also play an important primary part in degrading the elastic properties in bending of composites. Calculations of the reduced extensional and bending stiffness tensors of cross-ply laminates containing matrix cracks in the central 90° plies were performed by Ousset (1991), by derivation of a homogenized plate model. The obtained model possessed displacements of Kirchhoff–Love type, including three-dimensional stresses. Unfortunately, no explicit results were presented.

In the present paper, the reduced thermoelastic properties in extension and bending for composite laminates containing matrix cracks are calculated on the basis of the decrease in elastic energy due to the damage. Kirchhoff plate theory is adopted to predict the stresses prior to cracking in the plies of a laminate of arbitrary lay-up sequence. The elastic energy associated with the release of the stresses on the prospective crack surfaces is then calculated by use of solutions for the stress intensity factors for an array of cracks in an infinite homogenous medium. In this manner, the compliances, thermal expansion coefficients and eigenstrains due to the release of ply residual stresses are calculated.

2. THEORETICAL BASIS

2.1. Two-dimensional laminate theory for laminates without cracks

In order to facilitate the reading of the subsequent sections, the well-known two-dimensional laminate theory incorporating bending and extension will be briefly described. Assumptions associated with Kirchhoff plate theory will be adopted. In the following, characters with superscript letters denote local ply properties and characters with overbars denote global effective laminate properties. Matrix transpose will be indicated by a superscript 'T'. Consider a general two-dimensional laminate. The laminate consists of N plies, each of which is defined by a thickness t^k and ply material properties. In the thickness direction, ply k covers the distance between the coordinates h^{k-1} and h^k . The deformation of the laminate due to applied mechanical and thermal loads will be discussed in terms of the following quantities

$$\bar{\mathbf{P}} = \begin{pmatrix} \bar{\mathbf{N}} \\ \bar{\mathbf{M}} \end{pmatrix}, \quad \bar{\boldsymbol{\varepsilon}} = \begin{pmatrix} \bar{\boldsymbol{\varepsilon}} \\ \bar{\boldsymbol{\kappa}} \end{pmatrix}, \quad (1)$$

where the 3×1 vectors $\bar{\mathbf{N}}$ and $\bar{\mathbf{M}}$ are the familiar in-plane forces and moments per unit length and the corresponding vectors $\bar{\boldsymbol{\varepsilon}}$ and $\bar{\boldsymbol{\kappa}}$ are the in-plane strains and curvatures, respectively. Incorporating thermal expansion resulting from a homogeneous change in temperature ΔT , the global relation between the effective generalized stresses $\bar{\mathbf{P}}$ and strains $\bar{\boldsymbol{\varepsilon}}$ reads as

$$\bar{\boldsymbol{\varepsilon}} = \bar{\mathbf{S}}\bar{\mathbf{P}} + \bar{\mathbf{a}}\Delta T. \quad (2)$$

The components of the effective 6×6 laminate compliance matrix $\bar{\mathbf{S}}$ as well as of the 6×1 vector of thermal expansion coefficients $\bar{\mathbf{a}}$ remain to be determined. By adoption of the plane stress stiffness matrix \mathbf{Q}^k of ply k , the expression for the in-plane stresses $\boldsymbol{\sigma}^k = (\sigma_{11}^k, \sigma_{22}^k, \sigma_{12}^k)^T$ in ply k taking into account eventual residual stresses reads

$$\boldsymbol{\sigma}^k = \mathbf{Q}^k(\boldsymbol{\varepsilon}^k + (z - z^k)\boldsymbol{\kappa}^k - \boldsymbol{\alpha}^k \Delta T) + \boldsymbol{\sigma}_E^{k(R)} + \frac{2(z - z^k)}{t^k} \boldsymbol{\sigma}_B^{k(R)}, \quad (3)$$

where $\boldsymbol{\varepsilon}^k$ and $\boldsymbol{\kappa}^k$ are the average in-plane strains and midplane curvatures, respectively, of ply k . The current position in the thickness direction has been denoted as z , where the laminate midplane corresponds to $z = 0$. The residual stresses in the separate plies of the laminate may result from thermal or chemical anisotropic shrinkage during manufacturing. Effects of residual stresses are clearly visible in, for example, unsymmetric ($0^\circ/90^\circ$) laminates, which in most cases show considerable curvature after manufacturing. In the present model, the residual stress $\boldsymbol{\sigma}^{k(R)}$ in ply k has been assumed to be linearly varying and it is

described by the ply average residual stress $\sigma_E^{k(R)}$ and the residual stress amplitude $\sigma_B^{k(R)}$. The vector of in-plane thermal expansion in ply k is denoted as α^k . The midplane position z^k of ply k is introduced as

$$z^k = \frac{h^k + h^{k-1}}{2}. \quad (4)$$

For compatibility reasons, the ply mean strain ϵ^k and ply curvature κ^k can be determined from the corresponding effective laminate properties as $\epsilon^k = \bar{\epsilon} + z^k \bar{\kappa}$ and $\kappa^k = \bar{\kappa}$. The total laminate effective forces and moments per unit length can then be written as

$$\begin{aligned} \bar{\mathbf{N}} &= \bar{\mathbf{C}}_{EE} \bar{\boldsymbol{\epsilon}} + \bar{\mathbf{C}}_{EB} \bar{\boldsymbol{\kappa}} + \bar{\boldsymbol{\delta}}_E \Delta T, \\ \bar{\mathbf{M}} &= \bar{\mathbf{C}}_{BE} \bar{\boldsymbol{\epsilon}} + \bar{\mathbf{C}}_{BB} \bar{\boldsymbol{\kappa}} + \bar{\boldsymbol{\delta}}_B \Delta T. \end{aligned} \quad (5)$$

The subscripts 'E' and 'B' denote quantities associated with extension and bending, respectively. The effective stiffnesses and thermal stress coefficients for the uncracked laminate are, explicitly,

$$\begin{aligned} \bar{\mathbf{C}}_{EE} &= \sum_{k=1}^N t^k \mathbf{Q}^k, \\ \bar{\mathbf{C}}_{EB} = \bar{\mathbf{C}}_{BE} &= \sum_{k=1}^N t^k z^k \mathbf{Q}^k, \\ \bar{\mathbf{C}}_{BB} &= \sum_{k=1}^N t^k \left[(z^k)^2 + \frac{(t^k)^2}{12} \right] \mathbf{Q}^k \end{aligned} \quad (6)$$

and

$$\begin{aligned} \bar{\boldsymbol{\delta}}_E &= - \sum_{k=1}^N t^k \mathbf{Q}^k \boldsymbol{\alpha}^k, \\ \bar{\boldsymbol{\delta}}_B &= - \sum_{k=1}^N t^k z^k \mathbf{Q}^k \boldsymbol{\alpha}^k. \end{aligned} \quad (7)$$

The relations in eqn (5) may be inverted to acquire the effective compliances and thermal expansion coefficients for the uncracked laminate. The generalized extensions of the uncracked laminate may then be written

$$\begin{aligned} \bar{\boldsymbol{\epsilon}} &= \bar{\mathbf{S}}_{EE} \bar{\mathbf{N}} + \bar{\mathbf{S}}_{EB} \bar{\mathbf{M}} + \bar{\boldsymbol{\alpha}}_E \Delta T, \\ \bar{\boldsymbol{\kappa}} &= \bar{\mathbf{S}}_{BE} \bar{\mathbf{N}} + \bar{\mathbf{S}}_{BB} \bar{\mathbf{M}} + \bar{\boldsymbol{\alpha}}_B \Delta T. \end{aligned} \quad (8)$$

In deriving the above expressions for the total stiffnesses and total thermal stress coefficients, the fact has been exploited that the contributions from the residual stresses to the resulting laminate forces and moments per unit length must vanish.

2.2. Stiffnesses and thermal expansion coefficients of laminates containing matrix cracks

Consider a general two-dimensional laminate consisting of N laminae according to the previous subsection. A global coordinate system is defined by the axes X_1 and X_2 in the laminate plane and the axis X_3 pointing in the thickness direction. The axes Y_1^k , Y_2^k and Y_3^k define the local coordinate system in ply k . The fibres in ply k are aligned with the Y_1^k -axis, and the Y_2^k -axis defines the direction normal to the fibres but in the plane of the laminate. The axis Y_3^k is directed normal to the laminate plane and thus parallel to the axis X_3 . A state of damage in the form of transverse matrix cracks is assumed to prevail according

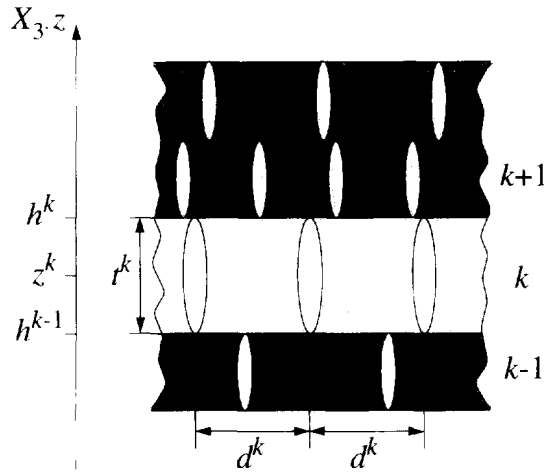


Fig. 1. A general two-dimensional laminate with a micro crack distribution. The damage state is determined by the crack densities $\rho^k = l^k / d^k$ in the separate plies.

to Fig. 1. In each ply, the cracks are presumed to be uniformly distributed and to be running in the local Y_1^k -direction. The crack state in ply k is determined from a crack density ρ^k defined as

$$\rho^k = \frac{l^k}{d^k}, \tag{9}$$

where d^k is the average distance between adjacent cracks in ply k . The presence of matrix cracks in one or several plies reduces the elastic energy of the laminate. This reduction in energy will be utilized to deduce the effective stiffnesses and compliances of the cracked laminate. The elastic energy W_0 that is stored in the uncracked laminate subjected to a prescribed generalized homogeneous extension $\bar{\epsilon}$ and change in temperature ΔT may be written as

$$W_0 = \frac{A}{2} (\bar{\epsilon} - \bar{\alpha} \Delta T)^T \bar{C} (\bar{\epsilon} - \bar{\alpha} \Delta T) + \sum_{k=1}^N f^k (\Delta T, \sigma^{k(R)}), \tag{10}$$

where A is the total in-plane area of the laminate and \bar{C} represents the 6×6 laminate effective stiffness matrix composed of the 3×3 stiffness matrices from eqn (6). The functions $f^k(\Delta T, \sigma^{k(R)})$ take into account the energy stored in the laminate due to interlaminar constraints, also when $\bar{\epsilon} - \bar{\alpha} \Delta T = \mathbf{0}$. The reduction in elastic energy resulting from the presence of cracks should be expressible in terms of the applied deformation $\bar{\epsilon}$. The elastic energy for the cracked laminate can be obtained from a superposition of (i) the energy of the uncracked laminate from eqn (10) and (ii) the change in elastic energy associated with the release of the stresses on the prospective crack surfaces. Problem two of the superposition thus corresponds to the application, with reversed sign, of the stresses calculated for the uncracked laminate onto the prospective crack surfaces under vanishing global displacements. As shown by Gudmundson and Östlund (1992a), the coupling terms between problems (i) and (ii) vanish.

Consider now the second problem of the superposition. Regard a single matrix crack in a typical ply k of the laminate positioned according to Fig. 2. The crack is loaded in the local Y_1^k - and Y_2^k -directions corresponding to mode III and mode I load types, respectively. The linearly varying in-plane stress σ^k from eqn (3) schematically depicted in Fig. 3(a) for both interior cracks and surface cracks is projected onto the prospective crack plane of ply k to form the 2×1 in-plane traction vectors τ_E^k and τ_B^k defined as

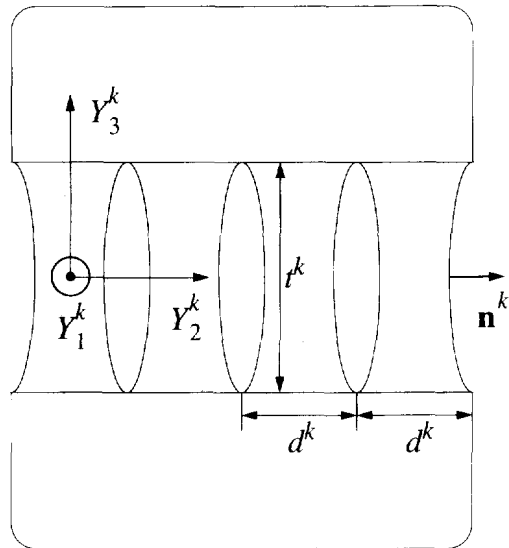


Fig. 2. A detailed view of an array of matrix cracks in a typical ply k of the laminate.

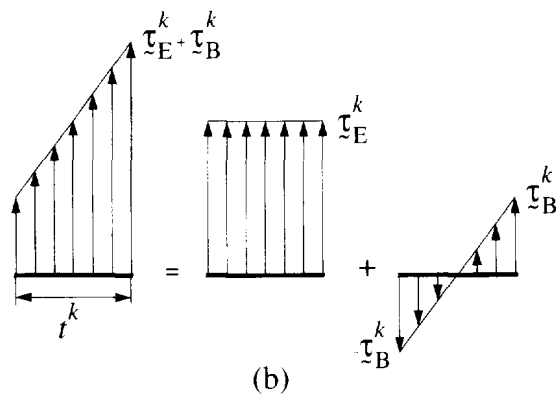
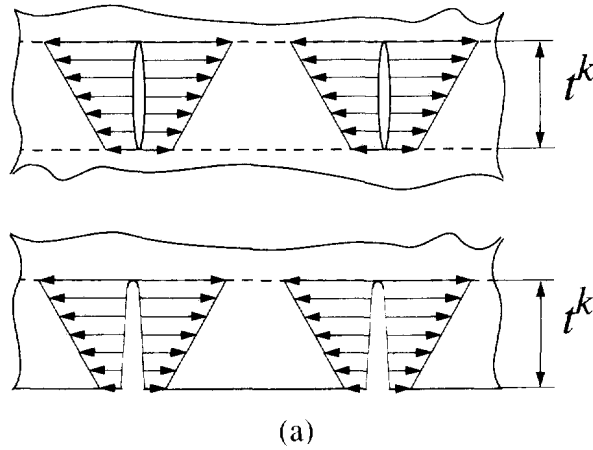


Fig. 3. (a) A schematic description of the stresses which are applied to the prospective crack surfaces in the second problem of the superposition. (b) The total traction vector in ply k is decomposed into the average traction τ_E^k and the traction amplitude vector τ_B^k .

$$\begin{aligned} \tau_E^k &= \mathbf{N}^k \mathbf{Q}^k (\bar{\epsilon} + z^k \bar{\kappa} - \alpha^k \Delta T) + \mathbf{N}^k \bar{\sigma}_E^{k(R)}, \\ \tau_B^k &= \frac{t^k}{2} \mathbf{N}^k \mathbf{Q}^k \bar{\kappa} + \mathbf{N}^k \bar{\sigma}_B^{k(R)}. \end{aligned} \tag{11}$$

The decomposition of the total traction vector in ply k which is required to form the vector of average tractions $\boldsymbol{\tau}_E^k$ and the traction amplitude vector $\boldsymbol{\tau}_B^k$ is illustrated in Fig. 3(b). The matrix \mathbf{N}^k is defined from the constant unit normal vector \mathbf{n}^k of the crack surfaces of ply k in accordance with Fig. 2. and reads

$$\mathbf{N}^k = \begin{pmatrix} n_1^k & 0 & n_2^k \\ 0 & n_2^k & n_1^k \end{pmatrix}. \quad (12)$$

Introducing the 4×4 matrices $\boldsymbol{\beta}^{kl}$ and the 4×1 vectors $\boldsymbol{\tau}^k$ as

$$\boldsymbol{\beta}^{kl} = \begin{pmatrix} \boldsymbol{\beta}_{EE}^{kl} & \boldsymbol{\beta}_{EB}^{kl} \\ \boldsymbol{\beta}_{BE}^{kl} & \boldsymbol{\beta}_{BB}^{kl} \end{pmatrix}, \quad \boldsymbol{\tau}^k = \begin{pmatrix} \boldsymbol{\tau}_E^k \\ \boldsymbol{\tau}_B^k \end{pmatrix}, \quad (13)$$

the work ΔW^k done by the tractions $\boldsymbol{\tau}^k$ on all crack surfaces in ply k may be expressed as

$$\Delta W^k = \frac{l^k \sqrt{l^k}}{2} (\boldsymbol{\tau}^k)^T \sum_{l=1}^N l^l \sqrt{l^l} \boldsymbol{\beta}^{kl} \boldsymbol{\tau}^l, \quad (14)$$

where l^k is the total crack length in ply k . The 2×2 submatrices $\boldsymbol{\beta}_m^{kl}$ ($m = EE, EB, BE, BB$) of the $\boldsymbol{\beta}^{kl}$ -matrices will be defined in the next section. The apparently arbitrarily chosen lengths in eqn (14) are introduced in order to enable convenient subsequent derivations. The length l^k is connected to the laminate in-plane area A and to the crack density ρ^k through

$$l^k = \frac{A \rho^k}{l^k}. \quad (15)$$

The contributions to the total crack surface work from all plies may now be added to obtain the total change in elastic energy ΔW as

$$\Delta W = \frac{A}{2} \sum_{k=1}^N \sum_{l=1}^N \sqrt{l^k \rho^k l^l \rho^l} (\boldsymbol{\tau}^k)^T \boldsymbol{\beta}^{kl} \boldsymbol{\tau}^l. \quad (16)$$

The total elastic energy $W_{(c)}$ for the cracked laminate is calculated by subtracting the crack surface work ΔW in eqn (16) from the energy W_0 valid for the uncracked laminate, so

$$W_{(c)} = \frac{A}{2} \left((\bar{\boldsymbol{\epsilon}} - \bar{\mathbf{a}} \Delta T)^T \bar{\mathbf{C}} (\bar{\boldsymbol{\epsilon}} - \bar{\mathbf{a}} \Delta T) - \sum_{k=1}^N \sum_{l=1}^N \sqrt{l^k \rho^k l^l \rho^l} (\boldsymbol{\tau}^k)^T \boldsymbol{\beta}^{kl} \boldsymbol{\tau}^l \right) + \sum_{k=1}^N f^k (\Delta T, \boldsymbol{\sigma}^{k(R)}). \quad (17)$$

For a cracked laminate in general, the following expression describes the elastic energy, provided that both thermal expansion and eigenstrains $\bar{\boldsymbol{\epsilon}}^{(R)}$ due to residual stresses are taken into account:

$$W_{(c)} = \frac{A}{2} (\bar{\boldsymbol{\epsilon}} - \bar{\mathbf{a}}_{(c)} \Delta T - \bar{\boldsymbol{\epsilon}}^{(R)})^T \bar{\mathbf{C}}_{(c)} (\bar{\boldsymbol{\epsilon}} - \bar{\mathbf{a}}_{(c)} \Delta T - \bar{\boldsymbol{\epsilon}}^{(R)}) + \sum_{k=1}^N g^k (\Delta T, \boldsymbol{\sigma}^{k(R)}). \quad (18)$$

Letters with subscript (c) indicate properties of the cracked laminate. Since eqns (17) and (18) represent two alternative ways of expressing the elastic energy of the damaged laminate, the stiffnesses, thermal expansion coefficients and eigenstrains of the cracked laminate can be obtained from an identification of terms using these two equations. To enable this, the

tractions τ^k in eqn (17) need to be expressed in terms of the generalized strain measures and residual stresses according to eqns (11) and (13). Identifying then terms containing the generalized strain vector $\bar{\mathbf{e}}$ yields the thermoelastic properties of the cracked laminate. By use of the matrices A_m^{kl} , defined as

$$\mathbf{A}_m^{kl} = \mathbf{Q}^k (\mathbf{N}^k)^T \boldsymbol{\rho}_m^{kl} \mathbf{N}^l \mathbf{Q}^l \quad m = \text{EE, EB, BE, BB}, \quad (19)$$

the changes $\Delta\bar{\mathbf{C}}$ and $\Delta\bar{\boldsymbol{\delta}}$ in stiffnesses and thermal stress coefficients along with the apparent forces $\bar{\mathbf{N}}^{(R)}$ and moments $\bar{\mathbf{M}}^{(R)}$ per unit length due to the release of residual stresses are introduced as

$$\Delta\bar{\mathbf{C}}_{\text{EE}} = - \sum_{k=1}^N \sum_{l=1}^N \sqrt{t^k \rho^k t^l \rho^l} \mathbf{A}_{\text{EE}}^{kl}, \quad (20a)$$

$$\Delta\bar{\mathbf{C}}_{\text{EB}} = \Delta\bar{\mathbf{C}}_{\text{BE}}^T = - \sum_{k=1}^N \sum_{l=1}^N \sqrt{t^k \rho^k t^l \rho^l} \left[z^l \mathbf{A}_{\text{EE}}^{kl} + \frac{t^l}{2} \mathbf{A}_{\text{EB}}^{kl} \right], \quad (20b)$$

$$\Delta\bar{\mathbf{C}}_{\text{BB}} = - \sum_{k=1}^N \sum_{l=1}^N \sqrt{t^k \rho^k t^l \rho^l} \left[z^k z^l \mathbf{A}_{\text{EE}}^{kl} + \frac{z^k t^l}{2} \mathbf{A}_{\text{EB}}^{kl} + \frac{z^l t^k}{2} \mathbf{A}_{\text{BE}}^{kl} + \frac{t^k t^l}{4} \mathbf{A}_{\text{BB}}^{kl} \right], \quad (20c)$$

$$\Delta\bar{\boldsymbol{\delta}}_{\text{E}} = \Delta\bar{\mathbf{C}}_{\text{EE}} \bar{\boldsymbol{\alpha}}_{\text{E}} + \Delta\bar{\mathbf{C}}_{\text{EB}} \bar{\boldsymbol{\alpha}}_{\text{B}} + \sum_{k=1}^N \sum_{l=1}^N \sqrt{t^k \rho^k t^l \rho^l} \mathbf{A}_{\text{EE}}^{kl} \boldsymbol{\alpha}^l, \quad (20d)$$

$$\Delta\bar{\boldsymbol{\delta}}_{\text{B}} = \Delta\bar{\mathbf{C}}_{\text{BE}} \bar{\boldsymbol{\alpha}}_{\text{E}} + \Delta\bar{\mathbf{C}}_{\text{BB}} \bar{\boldsymbol{\alpha}}_{\text{B}} + \sum_{k=1}^N \sum_{l=1}^N \sqrt{t^k \rho^k t^l \rho^l} \left[z^k \mathbf{A}_{\text{EE}}^{kl} + \frac{t^k}{2} \mathbf{A}_{\text{BE}}^{kl} \right] \boldsymbol{\alpha}^l, \quad (20e)$$

$$\bar{\mathbf{N}}^{(R)} = \sum_{k=1}^N \sum_{l=1}^N \sqrt{t^k \rho^k t^l \rho^l} \left[\mathbf{A}_{\text{EE}}^{kl} (\mathbf{Q}^l)^{-1} \boldsymbol{\sigma}_{\text{E}}^{(R)} + \mathbf{A}_{\text{EB}}^{kl} (\mathbf{Q}^l)^{-1} \boldsymbol{\sigma}_{\text{B}}^{(R)} \right], \quad (20f)$$

$$\bar{\mathbf{M}}^{(R)} = \sum_{k=1}^N \sum_{l=1}^N \sqrt{t^k \rho^k t^l \rho^l} \left[\left(z^k \mathbf{A}_{\text{EE}}^{kl} + \frac{t^k}{2} \mathbf{A}_{\text{BE}}^{kl} \right) (\mathbf{Q}^l)^{-1} \boldsymbol{\sigma}_{\text{E}}^{(R)} + \left(z^k \mathbf{A}_{\text{EB}}^{kl} + \frac{t^k}{2} \mathbf{A}_{\text{BB}}^{kl} \right) (\mathbf{Q}^l)^{-1} \boldsymbol{\sigma}_{\text{B}}^{(R)} \right]. \quad (20g)$$

The compliances, thermal expansion coefficients and generalized eigenstrains of the cracked composite laminate resulting from the identification between eqns (17) and (18) then read

$$\bar{\mathbf{S}}_{\text{EE}(c)} = [\bar{\mathbf{C}}_{\text{EE}} + \Delta\bar{\mathbf{C}}_{\text{EE}} - (\bar{\mathbf{C}}_{\text{EB}} + \Delta\bar{\mathbf{C}}_{\text{EB}}) (\bar{\mathbf{C}}_{\text{BB}} + \Delta\bar{\mathbf{C}}_{\text{BB}})^{-1} (\bar{\mathbf{C}}_{\text{BE}} + \Delta\bar{\mathbf{C}}_{\text{BE}})]^{-1}, \quad (21a)$$

$$\bar{\mathbf{S}}_{\text{EB}(c)} = \bar{\mathbf{S}}_{\text{BE}(c)}^T = - \bar{\mathbf{S}}_{\text{EE}(c)} (\bar{\mathbf{C}}_{\text{EB}} + \Delta\bar{\mathbf{C}}_{\text{EB}}) (\bar{\mathbf{C}}_{\text{BB}} + \Delta\bar{\mathbf{C}}_{\text{BB}})^{-1}, \quad (21b)$$

$$\bar{\mathbf{S}}_{\text{BB}(c)} = (\bar{\mathbf{C}}_{\text{BB}} + \Delta\bar{\mathbf{C}}_{\text{BB}})^{-1} + \bar{\mathbf{S}}_{\text{BE}(c)} \bar{\mathbf{S}}_{\text{EE}(c)}^{-1} \bar{\mathbf{S}}_{\text{EB}(c)}, \quad (21c)$$

$$\bar{\boldsymbol{\alpha}}_{\text{E}(c)} = \bar{\boldsymbol{\alpha}}_{\text{E}} - \bar{\mathbf{S}}_{\text{EE}(c)} \Delta\bar{\boldsymbol{\delta}}_{\text{E}} - \bar{\mathbf{S}}_{\text{EB}(c)} \Delta\bar{\boldsymbol{\delta}}_{\text{B}}, \quad (21d)$$

$$\bar{\boldsymbol{\alpha}}_{\text{B}(c)} = \bar{\boldsymbol{\alpha}}_{\text{B}} - \bar{\mathbf{S}}_{\text{BE}(c)} \Delta\bar{\boldsymbol{\delta}}_{\text{E}} - \bar{\mathbf{S}}_{\text{BB}(c)} \Delta\bar{\boldsymbol{\delta}}_{\text{B}}. \quad (21e)$$

$$\bar{\mathbf{e}}^{(R)} = \bar{\mathbf{S}}_{\text{EE}(c)} \bar{\mathbf{N}}^{(R)} + \bar{\mathbf{S}}_{\text{EB}(c)} \bar{\mathbf{M}}^{(R)}, \quad (21f)$$

$$\bar{\mathbf{k}}^{(R)} = \bar{\mathbf{S}}_{\text{BE}(c)} \bar{\mathbf{N}}^{(R)} + \bar{\mathbf{S}}_{\text{BB}(c)} \bar{\mathbf{M}}^{(R)}. \quad (21g)$$

The expressions in eqns (20) and (21) thus conclude the properties of the cracked laminate. From the compliances and thermal expansion coefficients in eqn (21), the reduced engineering constants for the cracked laminate are smoothly calculated. It can be noted that for vanishing coupling between extensions and curvatures, which is the case for a symmetric laminate, the in-plane properties $\bar{\mathbf{S}}_{\text{EE}(c)}$, $\bar{\boldsymbol{\alpha}}_{\text{E}(c)}$ and $\bar{\mathbf{e}}^{(R)}$ reduce to those of Gudmundson and Zang (1993).

2.3. The reduction in elastic energy associated with matrix cracks

Provided that the β^{kl} -matrices are known, the theory presented in the previous subsections offers the possibility to calculate the reduced compliances, thermal expansion coefficients and residual stress induced eigenstrains without invoking any approximations. Exact values of the β^{kl} -matrices are however impossible to derive, save for highly simplified cases. It is therefore necessary to derive approximate expressions for the dependency of the change in elastic energy on the applied crack surface tractions.

Gudmundson and Zang (1993) showed that such expressions for pure extension to a good accuracy can be obtained from the solutions for an array of cracks in an infinite or, for surface cracks, semi-infinite, homogeneous transversely isotropic body subjected to crack surface tractions as illustrated in Fig. 3(a). This observation will be utilized in the present work, and will be applied also to the crack surface tractions associated with bending. An implication of the approximation is that the different modes of crack opening displacements and crack surface tractions are independent. The 2×2 submatrices β_m^{kl} ($m = \text{EE, EB, BE, BB}$) of the β^{kl} -matrices then only have two non-vanishing components each, and may be written

$$\beta_m^{kl} = \begin{pmatrix} \beta_{11(m)}^{kl} & 0 \\ 0 & \beta_{22(m)}^{kl} \end{pmatrix} \quad m = \text{EE, EB, BE, BB}. \quad (22)$$

Further, the approximation mentioned above suggests that there will be no coupling between the crack opening displacements of different plies, hence

$$\beta^{kl} = \mathbf{0} \quad \text{for all } k \neq l. \quad (23)$$

To derive the expressions for the components of the β^{kl} matrices, the relation between the stress intensity factors and the energy release rate will be called upon. The cracks in the present problem are loaded by mode I and mode III type tractions. The traction vectors are, in accordance with the foregoing sections and Fig. 3(b), divided into one vector τ_E^k corresponding to constant tractions over the crack surface and a vector τ_B^k representing the linearly varying part of the tractions in ply k . The stress intensity factors K_I and K_{III} for the problem in Fig. 3(a), representing arrays of cracks in a homogeneous transversely isotropic medium are separated according to

$$\begin{aligned} K_{I(m)}(l^k) &= \tau_{2(m)}^k k_{2(m)} \sqrt{l^k} \\ K_{III(m)}(l^k) &= \tau_{1(m)}^k k_{1(m)} \sqrt{l^k} \end{aligned} \quad m = \text{E, B}, \quad (24)$$

where the traction vectors have been divided into their components $\tau_{1(m)}^k$ and $\tau_{2(m)}^k$ ($m = \text{E, B}$) in the local Y_1^k - Y_2^k -plane, and the ply thickness l^k serves as the current crack length. The non-dimensional parameters $k_{1(m)}$ and $k_{2(m)}$ ($m = \text{E, B}$) solely depend on the crack density. Given the stress intensity factors for a crack of arbitrary length x in ply k , the work ΔW^k done by the crack surface tractions for an array of cracks of total length l^k reads

$$\Delta W^k = l^k \int_0^{l^k} [\gamma_2^k (K_{I(E)}(x) + K_{I(B)}(x))^2 + \gamma_1^k (K_{III(E)}(x) + K_{III(B)}(x))^2] dx. \quad (25)$$

The quantities γ_1^k and γ_2^k are defined from the material properties of ply k as

$$\begin{aligned} \gamma_1^k &= \frac{1}{2G_{LT}^k}, \\ \gamma_2^k &= \frac{1 - \nu_{LT}^k \nu_{TL}^k}{E_T^k}. \end{aligned} \quad (26)$$

In eqn (26), ν_{LT}^k and ν_{TL}^k are the minor and major in-plane Poisson's ratios of the material in ply k , respectively. The in-plane shear modulus is denoted as G_{LT}^k and the transverse Young's modulus is indicated by E_T^k . With the help of eqn (25) the β^{kk} -matrices can be derived for both interior cracks and for surface cracks. Henceforth, a superscript (i) will indicate interior cracks and a superscript (s) will imply surface cracks.

For interior cracks, there will be no coupling between the extensional and bending components of the ply traction vector, i.e. $\beta_{EB}^{kk(i)}$ and $\beta_{BE}^{kk(i)}$ both vanish. The dimensionless stress intensity factors $k_{1(E)}^{(i)}$, $k_{2(E)}^{(i)}$ and $k_{1(B)}^{(i)}$ were obtained from Benthem and Koiter (1972) and Tada *et al.* (1973). The remaining quantity $k_{1(B)}^{(i)}$ corresponding to a linearly varying load in mode III could not be found in the literature, other than for a vanishing crack density. The energy associated with this type of loading was therefore numerically evaluated by use of the finite element method as described in Appendix A. The resulting expression for $k_{1(B)}^{(i)}$ is found in Appendix B. By use of eqns (14), (24) and (25), the sought matrix components can now be derived. The derivation is accounted for in Appendix B. The resulting components of the $\beta^{kk(i)}$ -matrices can be presented in the following form:

$$\begin{aligned}\beta_{11(EE)}^{kk(i)} &= \frac{\pi}{2} \gamma^k \frac{8}{(\pi \rho^k)^2} \ln \left[\cosh \left(\frac{\pi \rho^k}{2} \right) \right], \\ \beta_{22(EE)}^{kk(i)} &= \frac{\pi}{2} \gamma^k \sum_{i=1}^{10} \frac{a_i}{(1 + \rho^k)^i},\end{aligned}\quad (27)$$

for the components connected with pure extension and

$$\begin{aligned}\beta_{11(BB)}^{kk(i)} &= \frac{\pi}{16} \gamma^k \sum_{i=1}^{10} \frac{b_i}{(1 + \rho^k)^i}, \\ \beta_{22(BB)}^{kk(i)} &= \frac{\pi}{16} \gamma^k \sum_{i=1}^{10} \frac{c_i}{(1 + \rho^k)^i}\end{aligned}\quad (28)$$

for components which must be added to take bending into account. The curve fit parameters a_j , b_j and c_j are found in Table 1. The results in eqn (27) were obtained from Gudmundson and Zang (1993), whilst the expressions in eqn (28) were acquired by use of a least squares fit to the results from a numerical integration according to Appendix B.

For surface cracks there exists a coupling between the components of the traction vector associated with extension and bending. Care must also be devoted to the location of the crack tip in relation to the peak stress, which is insignificant for interior cracks. The expression in eqn (25) is still applicable, however. The non-dimensional stress intensity factors $k_{1(E)}^{(s)}$ and $k_{2(E)}^{(s)}$ for surface cracks were found in the papers by Benthem and Koiter (1972) and by Tada *et al.* (1973). The stress intensity factors $k_{1(B)}^{(s)}$ and $k_{2(B)}^{(s)}$ related to a linearly varying load were calculated from the numerically obtained elastic energies for

Table 1. The curve fit parameters used in eqns (27) and (28) determining the crack density dependence of the components of the matrices $\beta_{EE}^{kk(i)}$ and $\beta_{BB}^{kk(i)}$

j	a_j	b_j	c_j
1	0.63666	3.40409	1.65364
2	0.51806	-1.50821	0.87842
3	0.51695	-0.37842	10.61342
4	-1.04897	-3.62256	-135.67488
5	8.95572	-101.24283	747.53392
6	-33.09444	481.87306	-2236.32476
7	74.32002	-916.59087	3772.21227
8	-103.06411	898.56902	-3604.17159
9	73.60337	-452.85541	1827.29629
10	-20.34326	93.35216	-383.01680

closely related problems. This procedure is further explained in Appendix A. The obtained numerical expressions for the stress intensity factors corresponding to the linearly varying loads are elucidated in Appendix B, as are the integral expressions defining the components of the $\beta^{kk(s)}$ -matrices. The eventual explicit expressions for the matrix components for surface cracks are

$$\begin{aligned}\beta_{11(\text{EE})}^{kk(s)} &= \pi\gamma_1^k \frac{8}{(2\pi\rho^k)^2} \ln[\cosh(\pi\rho^k)], \\ \beta_{22(\text{EE})}^{kk(s)} &= 1.1215^2 \pi\gamma_2^k \sum_{j=1}^{10} \frac{d_j}{(1+\rho^k)^j}\end{aligned}\quad (29)$$

for the purely extensional load. The components in eqn (29) can be found in the paper by Gudmundson and Zang (1993). Incorporating also the fraction of the traction corresponding to bending, the following equations result

$$\begin{aligned}\beta_{11(\text{EB})}^{kk(s)} = \beta_{11(\text{BE})}^{kk(s)} &= -\frac{3\pi-8}{3} \gamma_1^k \sum_{j=1}^{10} \frac{e_j}{(1+\rho^k)^j}, \\ \beta_{22(\text{EB})}^{kk(s)} = \beta_{22(\text{BE})}^{kk(s)} &= -0.2364 \pi\gamma_2^k \sum_{j=1}^{10} \frac{f_j}{(1+\rho^k)^j}\end{aligned}\quad (30)$$

and

$$\begin{aligned}\beta_{11(\text{BB})}^{kk(s)} &= \frac{3\pi^2-16\pi+24}{3\pi} \gamma_1^k \sum_{j=1}^{10} \frac{g_j}{(1+\rho^k)^j}, \\ \beta_{22(\text{BB})}^{kk(s)} &= 0.1481 \pi\gamma_2^k \sum_{j=1}^{10} \frac{h_j}{(1+\rho^k)^j}.\end{aligned}\quad (31)$$

The fitted parameters d_j , e_j , f_j , g_j and h_j are found in Table 2. The components of the β^{kk} matrices given above are valid in the local coordinate system in ply k . For the calculation of the laminate properties according to eqns (20) and (21), the matrices of the different plies need to be transformed to a common coordinate system.

2.4. The reduction in elastic energy for an infinite crack density

In experimental investigations, it has come forward that matrix crack densities seldom exceed unity. Highsmith and Reifsnider (1982) reported of a saturated state with respect to crack density for cross-ply laminates subjected to both quasi-static and fatigue loads. The saturation state, named the characteristic damage state (CDS), in all cases accounted for revealed crack densities of the order of magnitude of unity. Having accepted these

Table 2. The curve fit parameters used in eqns (29), (30) and (31) determining the crack density dependence of the components of the matrices $\beta_m^{kk(s)}$ ($m = \text{EE, EB, BE, BB}$)

j	d_j	e_j	f_j	g_j	h_j
1	0.25256	-0.29208	-0.035206	2.00624	0.86388
2	0.27079	8.70026	0.97809	-2.57041	-2.87984
3	-0.49814	-82.11858	-7.58709	31.41892	34.19264
4	8.62962	479.23609	44.52217	-175.60882	-167.57885
5	-51.24655	-1633.39371	-150.85828	547.80573	458.21598
6	180.96305	3497.22398	333.94609	-1114.56953	-667.14207
7	-374.29813	-4751.26789	-487.71444	1494.40862	400.51994
8	449.59474	3954.62876	471.87242	-1256.18363	109.75154
9	-286.51016	-1835.18896	-273.59771	594.64188	-252.27544
10	73.84223	363.47237	69.47435	-120.34912	87.33293

experimental data, it might in any case be of interest to derive the thermoelastic properties of a composite laminate in which the crack densities tend to infinity. Especially for laminates containing surface cracks, the stiffnesses in pure extension come close to their values corresponding to an infinite crack density at moderately low crack densities, see, for example, Adolfsson and Gudmundson (1995). Reasonably, this effect is even more emphasised considering flexural stiffnesses due to the relatively larger importance of the top and bottom plies. By application of the approach outlined in the work by Gudmundson and Östlund (1992b), the energy associated with an infinite crack density is obtained, as are the matrix components

$$\begin{aligned}\beta_{11(EE)}^{kk(\text{inf})} &= \frac{2r_1^k}{\rho^k}, \\ \beta_{22(EE)}^{kk(\text{inf})} &= \frac{r_2^k}{\rho^k},\end{aligned}\quad (32)$$

for the traction corresponding to pure extension and as

$$\begin{aligned}\beta_{11(BB)}^{kk(\text{inf})} &= \frac{2r_1^k}{3\rho^k}, \\ \beta_{22(BB)}^{kk(\text{inf})} &= \frac{r_2^k}{3\rho^k}\end{aligned}\quad (33)$$

for the part of the ply traction representing the linearly varying part of the load. As can be seen from eqns (20) and (21), the crack density ρ^k which appears in eqns (32) and (33) will vanish in the final expressions for the compliances, thermal expansion coefficients and extra strains and curvatures due to the residual stresses. For infinite crack densities, there exists no need to distinguish between surface cracks and interior cracks, and the matrices $\beta_{EB}^{kk(\text{inf})}$ and $\beta_{BE}^{kk(\text{inf})}$ both vanish.

3. FINITE ELEMENT MODELLING

In order to check the accuracy and reliability of the approximate analytic method accounted for in the previous section, three-dimensional finite element calculations were performed for composite geometries containing different distributions of matrix cracks. The general purpose finite element code ABAQUS (1994) was utilized to calculate the thermoelastic properties of the laminates under consideration. The presented finite element model enables modelling of composite laminates containing an arbitrary number of plies with lay-up angles 0° , 90° , $+\theta$ and $-\theta$. Matrix cracks can then be positioned in an optional number of the included plies.

A periodic cell with an in-plane appearance according to Fig. 4 was identified and modelled with 20-noded isoparametric brick elements and 15-noded wedge elements. A sample periodic cell containing one of each of the four types of plies that can be modelled is shown in Fig. 5, where the possible crack surfaces are shaded. The effective compliances and thermal expansion coefficients of the cracked composite laminates were calculated from an evaluation of the average generalized strains resulting from an applied average generalized stress or temperature. The desired load is applied through the judicious application of displacement boundary conditions on the vertical outer boundary surfaces of the periodic cell. Utilizing the tensorial components $\bar{\epsilon}_{ij}$ and $\bar{\kappa}_{ij}$ of the effective laminate strain and curvature, respectively, the boundary conditions explicitly read as

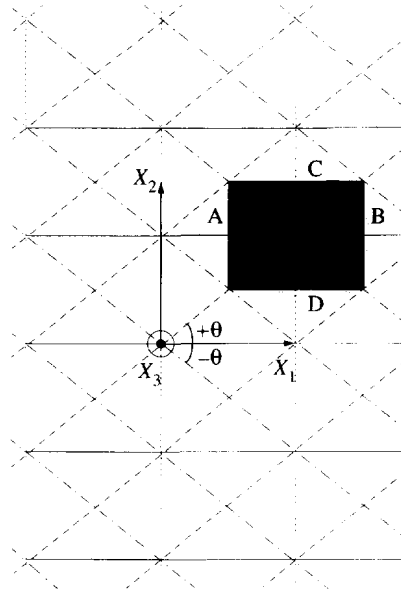


Fig. 4. A view in the negative X_3 -direction of the cracked laminate. The cracks in the 0° , 90° , θ and $-\theta$ plies are indicated by solid, dotted, dashed and dash-dotted lines, respectively. The identified unit cell is shaded. The vertical boundary surfaces of the unit cell are denoted by the letters A, B, C and D, respectively.

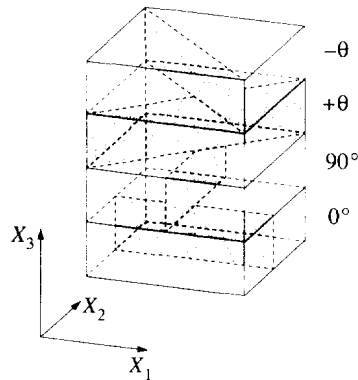


Fig. 5. A three-dimensional view of a sample unit cell containing the four types of plies which can be modelled by use of the presented finite element model. The prospective crack surfaces of each ply are shaded.

$$\begin{aligned}
 U_i^A - U_i^B &= (\bar{\epsilon}_{ij} + z^{AB} \bar{\kappa}_{ij})(X_j^A - X_j^B) \\
 U_i^C - U_i^D &= (\bar{\epsilon}_{ij} + z^{CD} \bar{\kappa}_{ij})(X_j^C - X_j^D)
 \end{aligned} \quad i, j = 1, 2, \tag{34}$$

where the coordinate pairs (X_j^A, X_j^B) and (X_j^C, X_j^D) correspond to equivalent points with respect to periodicity on the vertical boundary surfaces A, B and C, D according to Fig. 4. The in-plane displacements in the global coordinate system are denoted as U_1 and U_2 . As previously, z represents the current position in the thickness direction. Adopting instead a contracted notation for the strains and curvatures by reintroducing the 6×1 generalized strain vector $\bar{\epsilon}$ with the components $\bar{\epsilon}_i$, the boundary conditions in eqn (34) can be expressed as

$$\begin{aligned}
 U_i^A - U_i^B - H_{ij}^{AB} \bar{\epsilon}_j &= 0, \\
 U_i^C - U_i^D - H_{ij}^{CD} \bar{\epsilon}_j &= 0.
 \end{aligned} \tag{35}$$

In eqn (35), the components of the vectors $X_j^A - X_j^B$ and $X_j^C - X_j^D$ along with the dependency on the coordinate z have been collected in the 2×6 matrices H_{ij}^{AB} and H_{ij}^{CD} , respectively.

Control of the effective generalized strains can now be achieved by prescribing the six components in $\bar{\mathbf{e}}$ to six degrees of freedom not physically connected to the finite element model. From equivalence in energy, it follows that the resulting reaction forces in these six degrees of freedom are the generalized stresses averaged over the periodic cell times the volume of the cell. Vice versa, the six generalized stresses can be controlled by applying the desired stress or moment per unit area times the cell volume as a nodal load to the corresponding degree of freedom. The emanating displacements are then the correlative strains or curvatures. In this manner, by setting one of the controlled average generalized stresses to unity and suppressing the others, one column of the total effective 6×6 compliance matrix is obtained. This procedure is then repeated to cover all components of the compliance matrix. Analogously, the thermal expansion coefficients related to extension and bending can be evaluated as the displacements in the six crucial degrees of freedom resulting from application of a unit temperature in combination with vanishing global average stresses and moments.

Although the approximate analytic model proposed in the previous section is applicable to an arbitrary ply stacking sequence, the finite element cell used for verification obviously has its limitations. The main restriction clearly is that only four different lay-up angles can be modelled for a laminate. There are however also some restraints affecting the crack densities of the different plies of the laminate. From the picture of the periodic cell shown in Fig. 4, the following expressions connecting the different crack densities can be derived:

$$\begin{aligned}\rho^{90} &= \frac{t^{90}}{t^0} \rho^0 \tan \theta, \\ \rho^{7.0} &= \frac{t^{7.0}}{t^0} \rho^0 \cdot \frac{1}{\cos \theta}.\end{aligned}\quad (36)$$

Equation (36) thus states that there are only two independent parameters available for the in-plane design of the unit cell. These are the angle θ and the crack density ρ^0 , the latter of which is in essence a measure of the length of the unit cell in the X_2 -direction. The thicknesses of the separate plies of the representative cell can then be arbitrarily chosen, and cracks may be positioned in an arbitrarily chosen number of the included plies. The crack density of a certain ply thus either vanishes or is restricted by the expressions in eqn (36). Different crack densities are accomplished simply by changing the in-plane dimensions of the unit cell. The definition of the crack density also causes plies of the same lay-up angle but of different thicknesses to have different crack densities, since their in-plane dimensions are the same. It should be noted that although the restrictions described above exist, the model still offers the possibility of studying a rather wide range of different ply stacking sequences and crack density distributions.

4. RESULTS

Experimental reports concerning the effects of matrix cracking on the combined flexural and extensional stiffnesses of composite laminates with matrix cracks seem to be lacking in the literature. In order to calculate the residual stress induced eigenstrains $\bar{\mathbf{e}}^{(R)}$ and eigencurvatures $\bar{\mathbf{k}}^{(R)}$ according to eqns (21f) and (21g), the residual stresses $\sigma_E^{k(R)}$ and $\sigma_B^{k(R)}$ in the separate plies from manufacturing of the laminate need to be known. Such information may be obtained experimentally for a certain composite system and a certain curing procedure. Since the present investigation holds no experimental work, the verifications of the derived analytic expressions are performed by use of finite element results. Consequently, no information of the magnitude of ply residual stresses was available, and no examples of residual stress induced eigendeformations will be presented.

The thermoelastic properties of the cracked laminates will basically be presented in terms of the components of the 6×6 overall effective laminate compliance matrix and the 6×1 vector of thermal expansion coefficients. A transformation will be applied to ensure

Table 3. The characteristic engineering constants and thicknesses of the glass fibre reinforced epoxy (GFRP) ply and of the carbon fibre reinforced epoxy (CFRP) ply

Type	E_L (GPa)	E_T (GPa)	ν_{TL}	ν_{TT}	G_{LT} (GPa)	α_L (μK^{-1})	α_T (μK^{-1})	Ply thickness (mm)
GFRP	42	13	0.30	0.42	3.4	6.7	29	0.203
CFRP	145	9.6	0.31	0.46	4.8	-0.77	24	0.127

that all the presented properties are principally of the same dimension. A 6×6 compliance matrix $\hat{\mathbf{S}}_{(c)}$ is composed from the 3×3 compliance matrices of the cracked laminate previously seen. The matrix $\hat{\mathbf{S}}_{(c)}$ of equivalent laminate compliances is achieved by use of the total laminate thickness t as

$$\hat{\mathbf{S}}_{(c)} = \begin{pmatrix} t\bar{\mathbf{S}}_{EE(c)} & \frac{t^2}{2}\bar{\mathbf{S}}_{EB(c)} \\ \frac{t^2}{2}\bar{\mathbf{S}}_{BE(c)} & \frac{t^3}{12}\bar{\mathbf{S}}_{BB(c)} \end{pmatrix}. \quad (37)$$

Similarly, a 6×1 vector of equivalent thermal expansion coefficients $\hat{\boldsymbol{\alpha}}_{(c)}$ is introduced as

$$\hat{\boldsymbol{\alpha}}_{(c)} = \begin{pmatrix} \bar{\boldsymbol{\alpha}}_{E(c)} \\ \frac{t}{2}\bar{\boldsymbol{\alpha}}_{B(c)} \end{pmatrix}. \quad (38)$$

From the compliance matrix $\hat{\mathbf{S}}_{(c)}$, which is homogeneous with respect to dimension, the extensional and flexural moduli of the cracked composite are defined as

$$E_i = \frac{1}{\hat{S}_{ii(c)}}, \quad i = 1, 2, \dots, 6, \quad \text{no sum over } i. \quad (39)$$

The off-diagonal components of the compliance matrix $\hat{\mathbf{S}}_{(c)}$ will be displayed in terms of their ratios v_{ij} to the by column corresponding diagonal component, i.e.,

$$v_{ij} = \frac{\hat{S}_{ij(c)}}{\hat{S}_{jj(c)}}, \quad i, j = 1, 2, \dots, 6, \quad i \neq j, \quad \text{no sum over } j. \quad (40)$$

The thermal expansion coefficients will simply be expressed as the components α_i ($i = 1, 2, \dots, 6$) of the vector $\hat{\boldsymbol{\alpha}}_{(c)}$. It can be noted that for a symmetric laminate, the extensional moduli E_1 , E_2 and E_3 reduce to the ordinary in-plane E -moduli and shear modulus, respectively. When possible, the presented thermoelastic properties are normalized by division by their corresponding values for the uncracked laminate. If the displayed laminate property vanishes for the virgin laminate, the absolute value of the property is presented. Five sample types of laminate will be examined: symmetric and unsymmetric cross-ply laminates, unsymmetric angle ply laminates, a quasi-isotropic laminate and a laminate of a more general lay-up of the type $(90^\circ / -55^\circ / 0^\circ / -55^\circ / 90^\circ / 55^\circ / 0^\circ)$. The material properties are chosen as typical values for glass fibre reinforced epoxy (GFRP) and for carbon fibre reinforced epoxy (CFRP), respectively. The carbon reinforced epoxy exhibits a higher degree of orthotropy in both elastic and thermal properties. The utilized material properties and ply thicknesses for the two different composite systems are found in Table 3. The engineering constants for the examined laminate types in their virgin states

Table 4. The equivalent extensional and flexural moduli of the investigated laminates in their virgin states

Laminate	Extensional moduli			Flexural moduli		
	E_1 (GPa)	E_2 (GPa)	E_3 (GPa)	E_4 (GPa)	E_5 (GPa)	E_6 (GPa)
GFRP (0 ₂ /90 ₃ /0 ₁) ₃	27.6	27.6	3.40	33.6	21.5	3.40
GFRP (90°/0°) ₃	26.9	26.9	3.40	26.9	26.9	3.40
GFRP (0°/90°/+45°/-45°) ₃	20.9	20.9	7.73	30.0	22.0	4.45
CFRP (-67.5°/67.5°) ₃	9.89	78.2	19.8	9.89	78.2	19.8
CFRP (90°/-55°/0 ₂ /-55 ₂ /90°/55 ₂ /0°) ₃	52.4	50.6	15.4	58.7	57.7	11.9

Table 5. The extensional and flexural ratios of the investigated laminates in their virgin states

Laminate	Extensional ratios			Flexural ratios		
	ν_{23}	ν_{13}	ν_{12}	ν_{56}	ν_{46}	ν_{45}
GFRP (0 ₂ /90 ₃ /0 ₁) ₃	0	0	0.143	0	0	0.117
GFRP (90°/0°) ₃	0	0	0.143	0	0	0.143
GFRP (0°/90°/+45°/-45°) ₃	0	0	0.350	0	0	0.160
CFRP (-67.5°/67.5°) ₃	0	0	1.38	0	0	1.38
CFRP (90°/-55°/0 ₂ /-55 ₂ /90°/55 ₂ /0°) ₃	-0.0732	-0.0524	0.185	0.0344	-0.0146	0.147

are found in Tables 4–7. At most, 21 independent and non-vanishing components of the compliance matrix along with 6 thermal expansion coefficients are obtained for a laminate. In order to reduce the amount of data presented, for the major part of the considered laminates some of the thermoelastic properties are omitted in the subsequent figures. The accuracies in the compliances and thermal expansion coefficients which are left out are, however, of the same order of magnitude as in those presented.

4.1. Cross-ply laminates

An important special case of the angle ply laminates are the cross-ply laminates, characterized by a stacking of 0° and 90° plies. The extensional stiffnesses and to some extent also the thermal expansion coefficients of cross-ply laminates containing matrix cracks have been thoroughly examined over the past years. The review article by Abrate (1991) may serve as a source for further information on this topic. In the present investigation, two types of cross-ply laminates will be examined. The two types are the symmetric

Table 6. The extensional–flexural coupling ratios of the investigated laminates in their virgin states. Only the laminates which exhibit a flexural–extensional coupling are included in this table

Laminate	Extensional–flexural ratios								
	ν_{14}	ν_{15}	ν_{16}	ν_{24}	ν_{25}	ν_{26}	ν_{34}	ν_{35}	ν_{36}
GFRP (90°/0°) ₃	0.262	0	0	0	-0.262	0	0	0	0
CFRP (-67.5°/67.5°) ₃	0	0	0.0340	0	0	0.178	0.0170	0.703	0
CFRP (90°/-55°/0 ₂ /-55 ₂ /90°/55 ₂ /0°) ₃	0.0951	0.139	0.115	0.129	-0.258	0.352	0.506	1.09	0.282

Table 7. The equivalent extensional and flexural thermal expansion coefficients of investigated laminates in their virgin states

Laminate	Extensional TECs			Flexural TECs		
	α_1 (μK^{-1})	α_2 (μK^{-1})	α_3 (μK^{-1})	α_4 (μK^{-1})	α_5 (μK^{-1})	α_6 (μK^{-1})
GFRP (0 ₂ /90 ₃ /0 ₁) ₃	12.8	12.8	0	0	0	0
GFRP (90°/0°) ₃	13.1	13.1	0	-4.16	4.16	0
GFRP (0°/90°/+45°/-45°) ₃	12.8	12.8	0	0	0	0
CFRP (-67.5°/67.5°) ₃	19.6	-3.27	0	0	0	-2.77
CFRP (90°/-55°/0 ₂ /-55 ₂ /90°/55 ₂ /0°) ₃	1.99	2.17	2.12	0.991	0.533	-10.1

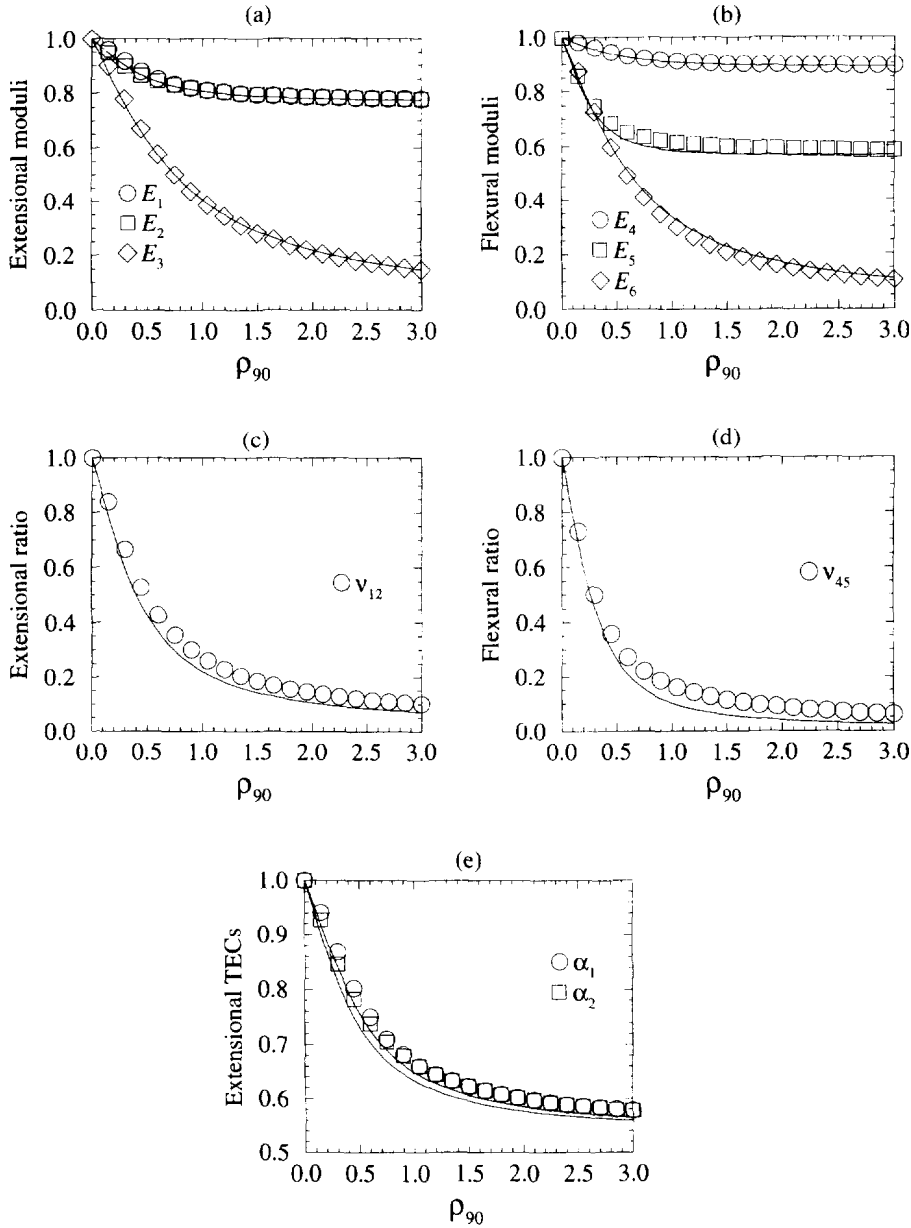


Fig. 6. The reduced engineering constants of the symmetric balanced $(0_2/90_3/0)_s$ GFRP laminate. The analytic results are indicated by lines and the finite element results by symbols. The symbols and the solid lines indicate the thermoelastic properties for the laminate with cracks in all plies. All the presented properties have been normalized by division by the equivalent properties for the virgin laminate.

$(0_2/90_3/0)_s$ GFRP laminate and the non-symmetric $(90/0)_3$ GFRP laminate. The non-symmetric lay-up will induce a coupling between the extensional and flexural compliances and thermal expansion coefficients. The symmetric lay-up will not exhibit this coupling.

The thermoelastic properties of the symmetric $(0_2/90_3/0)_s$ GFRP laminate are displayed in Fig. 6. The symbols and the solid lines show the thermoelastic properties when both the 90° plies and the 0° plies contain cracks, thus incorporating also surface cracks. Due to the symmetric lay-up, all the coefficients of flexural thermal expansion vanish.

Figure 7 reveals the compliances and thermal expansion coefficients of the balanced but not symmetric $(90^\circ/0^\circ)_3$ GFRP laminate. In this picture, the symbols and the solid lines indicate the characteristics of the laminate with cracks present in all plies. The non-symmetric lay-up unmasks its character by the non-vanishing extensional–flexural ratios seen in Fig. 7(c) and (d). The properties of these two sub-figures have not been normalized, as opposed to the other quantities presented. The lack of symmetry also produces the

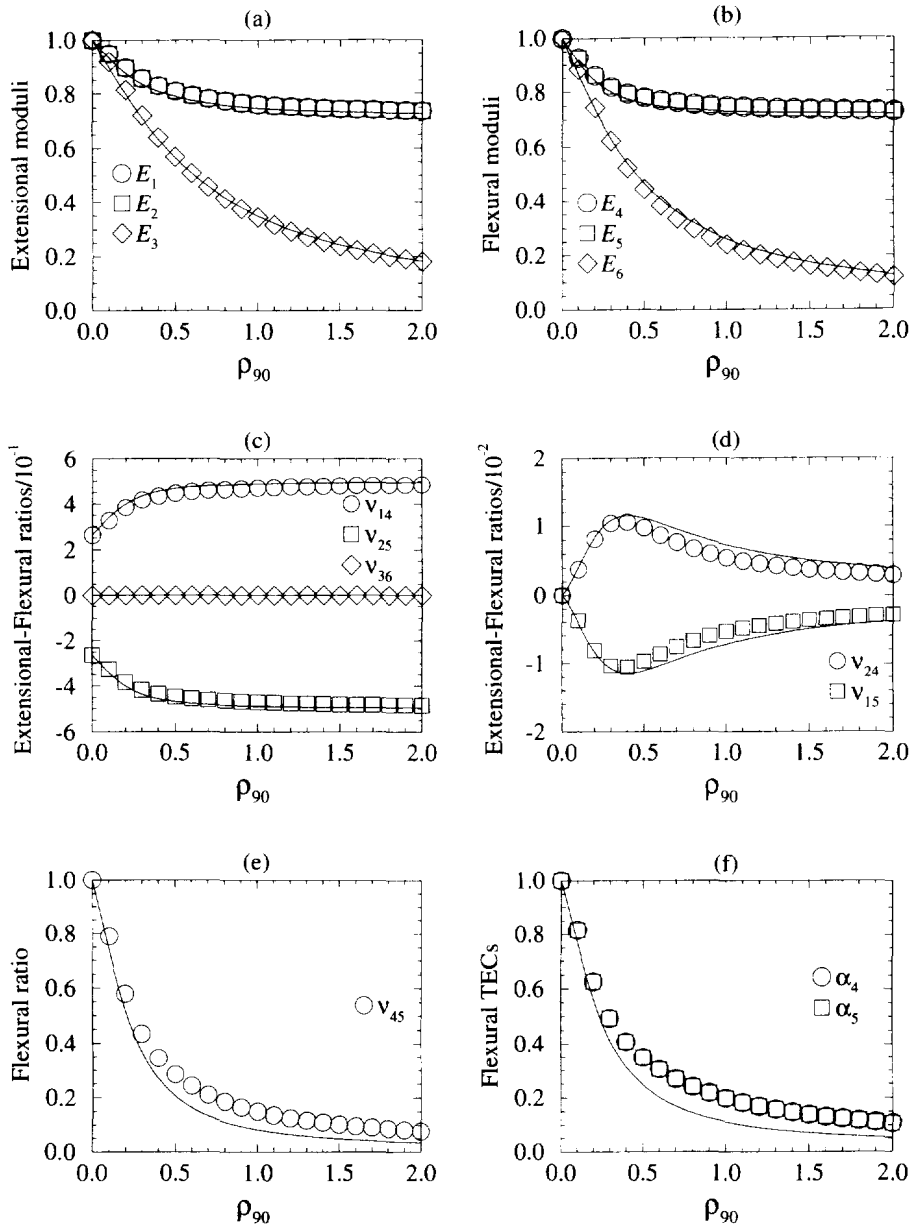


Fig. 7. The reduced engineering constants of the unsymmetric balanced $(90/0)_3$ GFRP laminate. The analytic results are indicated by lines and the finite element results by symbols. The symbols and the solid lines indicate the thermoelastic properties for the laminate with cracks in all plies. All the presented properties except the extensional–flexural ratios in Fig. 7(c) and (d) have been normalized by division by the equivalent properties for the virgin laminate.

flexural thermal expansion coefficients in Fig. 7(f). In both Fig. 6 and Fig. 7, the agreement between the approximate analytic results and the finite element results is fairly good.

4.2. Quasi-isotropic laminate

The reduced engineering properties for an initially extensionally quasi-isotropic symmetric $(0^\circ/90^\circ/+45^\circ/-45^\circ)_s$ GFRP laminate are shown in Fig. 8. The results are valid for a laminate with matrix cracks in all plies. Normalization has been applied to all the presented properties except those of Fig. 8(e). The straight lines shown in Fig. 8(a)–(f) are the corresponding properties for an infinite crack density calculated by use of eqns (32) and (33). Since symmetry prevails for all crack densities, extensional–flexural coupling will

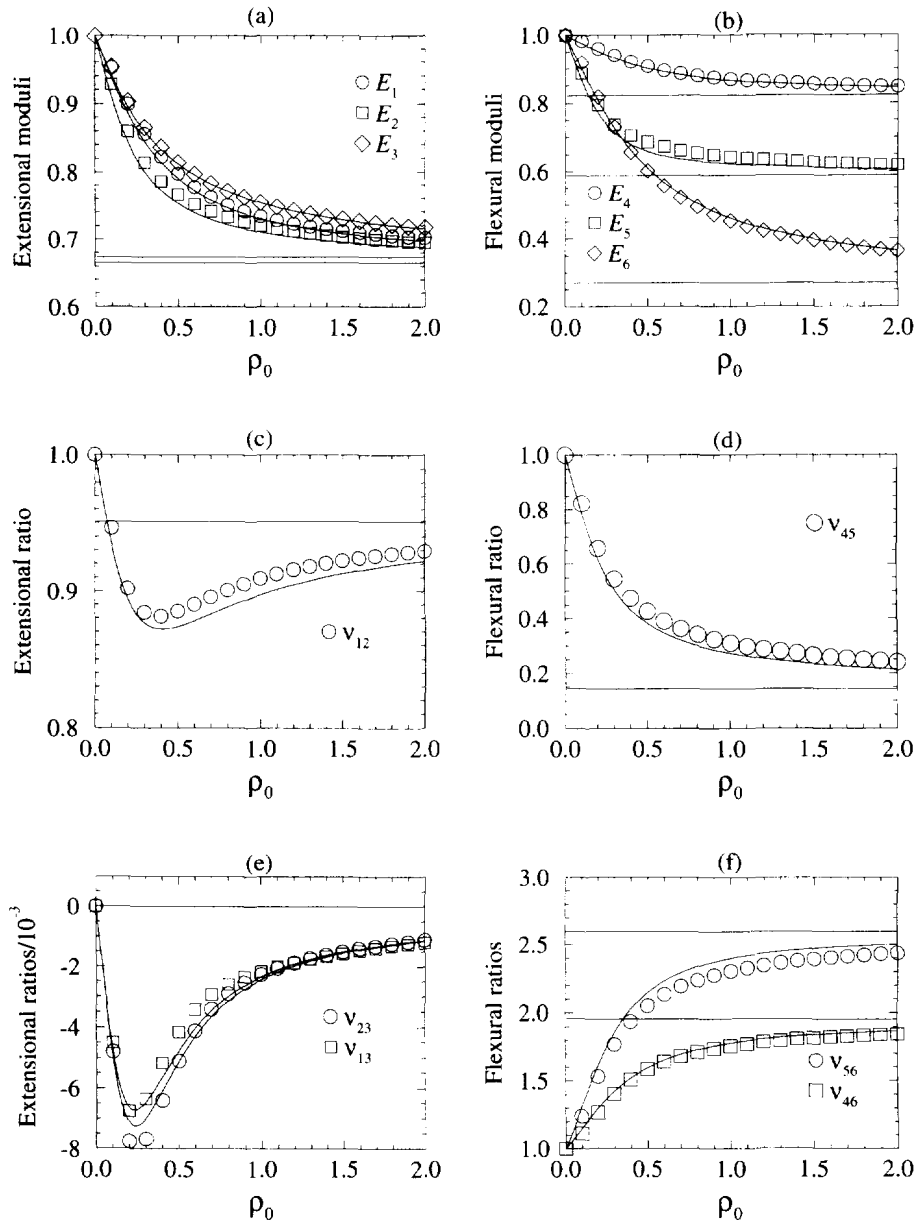


Fig. 8. The reduced engineering constants of the symmetric balanced quasi-isotropic ($0^\circ/90^\circ/+45^\circ/-45^\circ$)₃ GFRP laminate. The laminate exhibits cracks in all plies. The analytic results are indicated by lines and the finite element results by symbols. The straight lines indicate the elastic properties for an infinite crack density. All the presented properties except the extensional ratios v_{23} and v_{13} in Fig. 8(e) have been normalized by division by the equivalent properties for the virgin laminate.

occur neither in the stiffness properties nor in the thermal properties. Since the 0° plies serve as upper and lower laminae in the present laminate, the reductions in the flexural moduli E_5 corresponding to an applied bending moment m_{22} per unit area are significantly larger than those of the flexural moduli E_4 . This effect is clearly visible in Fig. 8(b). The corresponding extensional moduli E_1 and E_2 , however, for high crack densities approach the same level. Figure 8(f) reveals that the coupling between twist and flex, represented by the parameters v_{56} and v_{46} , increases with an increasing crack density.

4.3. Angle ply laminates

The characteristic thermoelastic properties of a CFRP ($-67.5^\circ/67.5^\circ$)₃ angle ply laminate with cracks exclusively in the 67.5° plies are shown in Fig. 9. The straight lines give

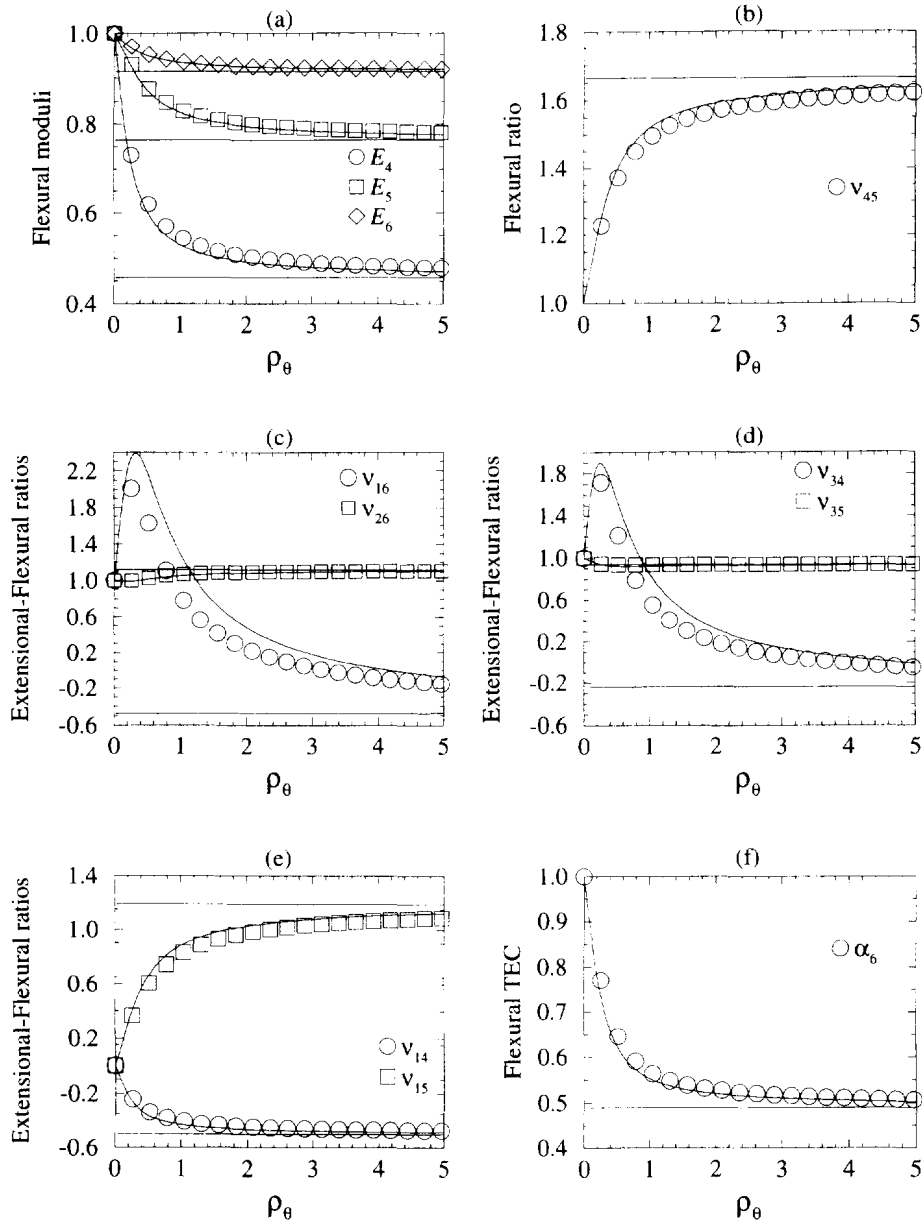


Fig. 9. The reduced engineering constants of the CFRP $(-67.5/67.5)_3$ angle ply laminate with cracks in the 67.5 plies. The analytic results are indicated by lines and the finite element results by symbols. All the presented properties except the extensional and flexural ratios in Fig. 9(e) have been normalized by division by the equivalent properties for the virgin laminate.

the corresponding properties for an infinite crack density. It can be noted that for the major part of the presented thermoelastic properties, good agreement holds between the numerically and analytically obtained results. The largest discrepancies are found for the extensional–flexural ratios in Fig. 9(c) and (d).

4.4. An unbalanced and unsymmetric laminate

The thermoelastic properties of an unbalanced and unsymmetric $(90^\circ/-55^\circ/0_2/-55^\circ/90^\circ/55^\circ/0)$ CFRP laminate containing matrix cracks in all plies are presented in Fig. 10. For this laminate type, exhibiting neither symmetry nor balance, none of the components of the compliance tensor nor of the vector of thermal expansion vanish for the virgin laminate. The largest differences between the analytic and numeric results are found for the flexural thermal expansion coefficients in Fig. 10(f).

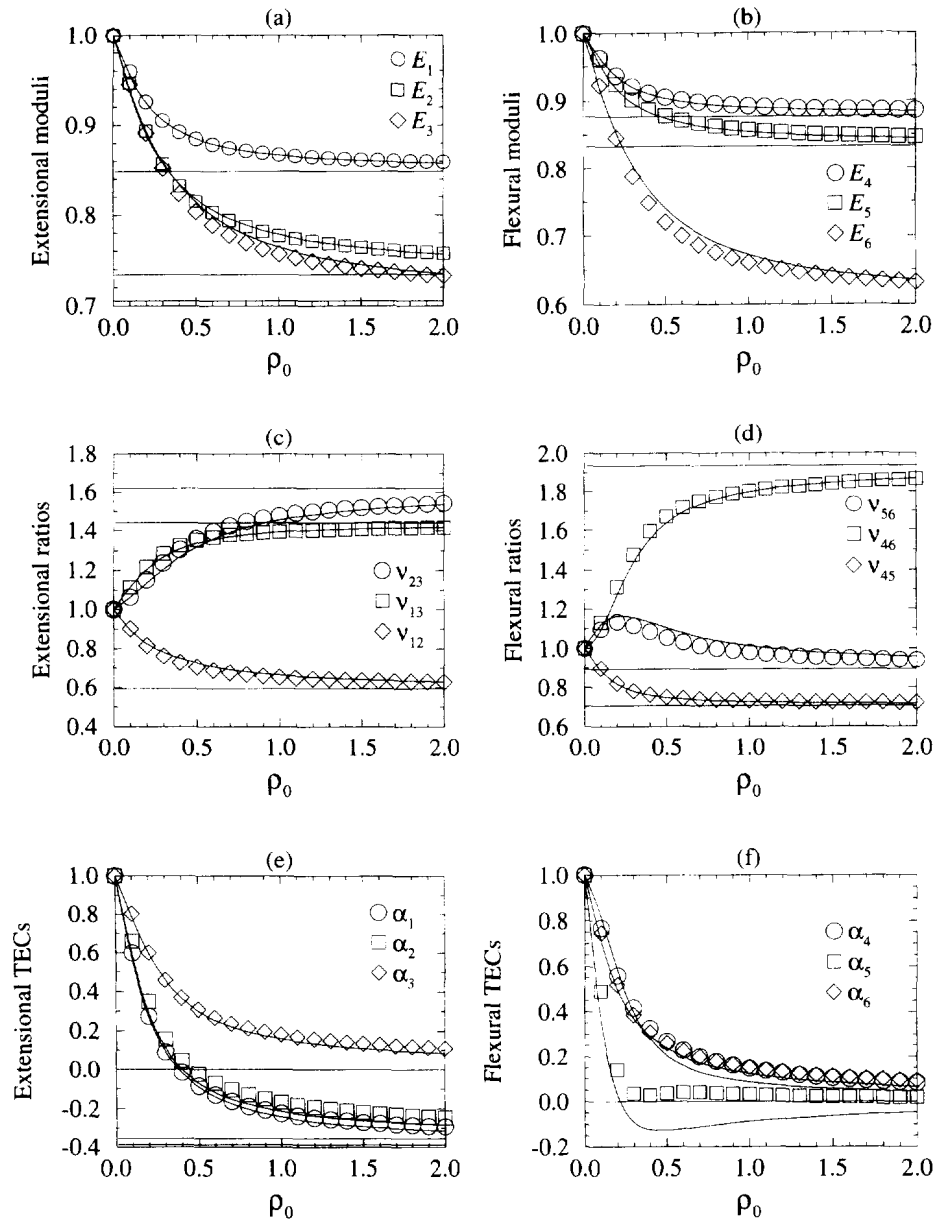


Fig. 10. The reduced engineering constants of the $(90_{-55} / 0_2 / -55_2 / 90_{.55} / 0)$ CFRP laminate with cracks in all plies. The symbols represent the finite element results and the solid lines indicate the approximate analytic results. The straight solid lines show the thermoelastic properties corresponding to infinite crack densities in all plies. All the presented properties have been normalized by division by the equivalent properties for the virgin laminate.

5. DISCUSSION

A model for the thermoelastic properties of composite laminates in combined bending and extension has been presented. The model can handle thin laminates of arbitrary ply stacking sequences and optional crack densities. Expressions for the thermoelastic properties of laminates containing an infinite number of cracks in specified laminates have also been derived. No experimental data other than ply material properties like E -moduli, Poisson's ratios and thermal expansion coefficients are required for the application of the presented method.

The results which have been presented in the previous sections are based on the stress intensity factors for an array of cracks in an infinite homogenous isotropic body. These solutions are then applied to geometries and materials which deviate considerably from the ones originally addressed. The errors thus introduced have, however, proven to be small for the investigated laminate geometries.

For extremely thin laminates, containing, for example, only two plies, which then both experience surface cracks, the changes in thermoelastic properties with increasing crack density are very rapid for low crack densities. For these laminates, the stiffnesses and thermal expansion coefficients valid for infinite crack densities can be rightly applied even at moderately high crack densities, such as the characteristic damage state (CDS) described by Highsmith and Reifsnider (1982).

The thermoelastic properties displayed in the present paper have been derived regardless of the phenomenon of matrix crack closure, liable to appear in composite bending. Including crack closure would result in higher calculated stiffnesses of the laminate, and would also induce non-linearities in the generalized global stress-strain relations. It would also be valuable to combine the presented model with a crack initiation and growth criterion to enable prediction of damage development. The incorporation of crack closure and damage evolution is left for future developments.

REFERENCES

- ABAQUS User's manual version 5.4 (1994). Hibbit, Karlsson and Sorensen, Inc., Pawtucket, RI.
- Abrate, S. (1991). Matrix cracking in laminated composites: a review. *Computers in Engineering* **1**, 337-353.
- Adolfsson, E. and Gudmundson, P. (1995). Matrix crack induced stiffness reductions in $[(0_m, 90_n, +\theta_p, -\theta_q)_s]_m$ composite laminates. *Computers in Engineering* **5**, 107-123.
- Aveston, J. and Kelly, A. (1973). Theory of multiple fracture of fibrous composites. *Journal of Material Science* **8**, 352-362.
- Benthem, J. P. and Koiter, W. T. (1972). Asymptotic approximations to crack problems. In *Mechanics of Fracture 1: Methods of Analysis and Solutions of Crack Problems* (ed. G. C. Sih), pp. 131-178. Noordhoff International Publishers, Leyden, The Netherlands.
- Choi, H. T., Wang, H. S. and Chang, F.-K. (1992). Effect of laminate configuration and impactor's mass on the initial impact damage of graphite/epoxy composite plates due to line-loading impact. *Journal of Computers and Materials* **26**, 804-827.
- Choi, H. T., Wu, H. Y. T. and Chang, F. K. (1991a). A new approach toward understanding damage mechanics and mechanics of laminated composites due to low-velocity impact. Part I—Experiments. *Journal of Computers and Materials* **25**, 992-1011.
- Choi, H. T., Wu, H. Y. T. and Chang, F. K. (1991b). A new approach toward understanding damage mechanics and mechanics of laminated composites due to low-velocity impact, Part II—Analysis. *Journal of Computers and Materials* **25**, 1012-1038.
- Gottesman, T., Hashin, Z. and Brull, M. A. (1980). Effective elastic moduli of cracked fibre composites. In *Advances in Composite Materials, Proceedings of the Third International Conference in Composite Materials* (eds A. R. Bunsell et al.), Vol. 1, pp. 749-758. Pergamon Press, Oxford, England.
- Gudmundson, P. and Östlund, S. (1992a). First order analysis of stiffness reduction due to matrix cracking. *Journal of Computers and Materials* **26**, 1009-1030.
- Gudmundson, P. and Östlund, S. (1992b). Prediction of thermoelastic properties of composite laminates with matrix cracks. *Computers in Science and Technology* **44**, 95-105.
- Gudmundson, P. and Zang, W. (1993). An analytic model for the thermoelastic properties of composite laminates containing transverse matrix cracks. *International Journal of Solids and Structures* **30**, 3211-3231.
- Hahn, H. T. and Tsai, S. W. (1974). On the behavior of composite laminates after initial failures. *Journal of Computers and Materials* **8**, 288-305.
- Highsmith, A. L. and Reifsnider, K. L. (1982). Stiffness-reduction mechanisms in composite laminates. In *Damage in Composite Materials, ASTM STP 775* (ed. K. L. Reifsnider), pp. 103-117. American Society for Testing and Materials, Philadelphia, PA.
- Hong, S. and Liu, D. (1989). On the relationship between impact energy and delamination area. *Experimental Mechanics*, June, 115-120.
- Jamison, R. D. and Reifsnider, K. L. (1982). Advanced fatigue damage development in graphite epoxy laminates. *Report AFWAL TR-82-3103*, Virginia Polytechnic Institute and State University, Blacksburg, VA.
- Kwon, Y. W. and Weiseman, K. (1991). Study of flexural stiffness in delaminated composite plates. In *Composite Material Technology 1991, PD-Vol. 37*. Proceedings of the Fourteenth Annual Energy-sources Technology Conference and Exhibition, Houston, TX (ed. D. Hui), pp. 101-103. The American Society of Mechanical Engineers, New York, NY.
- Lim, S. G. and Hong, C. S. (1989). Prediction of transverse cracking and stiffness reduction in cross-ply laminated composites. *Journal of Computers and Materials* **23**, 695-713.
- Liu, S., Kutlu, Z. and Chang, F.-K. (1993). Matrix cracking and delamination in laminated composite beams subjected to a transverse concentrated line load. *Journal of Computers and Materials* **27**, 436-470.
- Liu, D. and Malvern, L. M. (1987). Matrix cracking in impacted glass epoxy plates. *Journal of Computers and Materials* **21**, 594-609.
- Masters, J. E. Jr. (1981). An experimental investigation of cumulative damage development in graphite epoxy laminates. Ph.D. thesis, Virginia Polytechnic Institute and State University, Blacksburg, VA.
- Östlund, S. and Gudmundson, P. (1992). Numerical analysis of matrix-crack-induced delaminations in $[\pm 55]$ GFRP laminates. *Computers in Engineering* **2**, 161-175.
- Ousset, Y. (1991). Modèle homogénéisé d'une plaque composite présentant de la fissuration transverse. *La Recherche Aérospatiale*, **3**, 33-47.

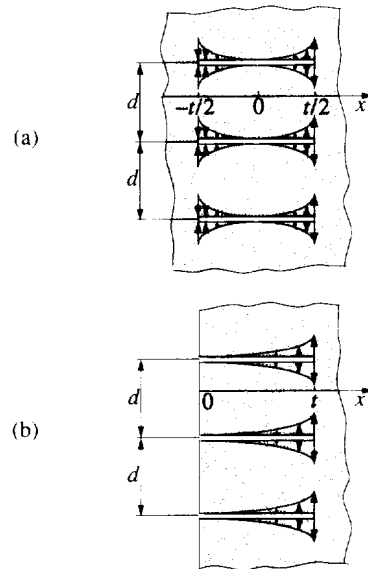


Fig. A1. (a) An array of interior cracks in an infinite body and (b) an array of surface cracks in a semi-infinite body. The crack surfaces are subjected to varying tractions.

- Reifsnider, K. L. (1977). Some fundamental aspects of the fatigue and fracture response of composite materials. In *Proc. 14th Ann. Soc. Engng Sci. Meeting*, Lehigh University, 14–16 Nov. 1977, pp. 373–384, Bethlehem, PA.
- Sendeckyj, G. P., Richardson, M. D. and Pappas, J. E. (1974). Fracture behavior of Thorne 300/5208 graphite-epoxy laminates—Part I: Unnotched laminates. In *Composite Reliability*, ASTM STP 580 (ed. E. M. Wu), pp. 528–546, American Society for Testing and Materials, Philadelphia, PA.
- Tada, H., Paris, P. C. and Irwin, G. R. (1985). *The Stress Analysis of Cracks Handbook*, (2nd edition), Paris Productions Incorporated (and Del Research Corporation), St. Louis, MO.
- Talreja, R. (1985). Transverse cracking and stiffness reduction in composite laminates. *Journal of Computers and Materials* **19**, 355–375.
- Tracy, J. J. and Pardo, G. C. (1988). Effect of delamination on the flexural stiffness of composite laminates. *Thin-Walled Structures* **6**, 371–383.
- Tsangarakis, N. and Taleghani, B. K. (1995). Biaxial flexural testing of a carbon fiber reinforced epoxy composite. *Journal of Computers and Materials* **29**, 1359–1373.
- Xu, L.-Y. (1995). Influence of stacking sequence on the transverse matrix cracking in continuous fibre crossply laminates. *Journal of Computers and Materials* **29**, 1337–1358.

APPENDIX A

Consider an array of interior cracks of length t according to Fig. A1(a) or a similar array of surface cracks of length t in accordance with Fig. A1(b). The extension of the cracks in the direction perpendicular to the plane of the paper is l . The crack surfaces are subjected to varying stresses. The stress $\tau(x)$ varies along the length t of the cracks as

$$\tau(x) = \sigma \cdot \left(\frac{2x}{t} \right)^n \quad (\text{A1})$$

for the interior cracks and as

$$\tau(x) = \sigma \cdot \left(\frac{x}{t} \right)^n \quad (\text{A2})$$

for the surface cracks. In eqns (A1) and (A2), the parameter n is a non-negative integer. The distance between adjacent cracks is d . The crack density ρ is defined as

$$\rho = \frac{t}{d}. \quad (\text{A3})$$

The stress intensity factor $K(t)$ for the present case, be it in mode I, II or III, can be written as

$$K(t) = \sigma k(\rho) \sqrt{t}. \quad (\text{A4})$$

where the non-dimensional factor $k(\rho)$ accommodates the crack density dependency. By use of the relation between the stress intensity factor and the energy release rate \dot{G} .

$$G = \gamma K^2, \quad (\text{A5})$$

and the relation between the elastic energy W in the region corresponding to a single crack and the energy release rate,

$$G = \frac{1}{l} \frac{\partial W}{\partial t}, \quad (\text{A6})$$

the elastic energy W may be evaluated as

$$W(t, d) = l \int_0^r [K(x)]^2 dx, \quad (\text{A7})$$

or explicitly

$$W(t, d) = \frac{l \sigma^2}{t^{2n}} \int_0^r x^{2n-1} \left[k \left(\frac{x}{t} \rho \right) \right]^2 dx. \quad (\text{A8})$$

By differentiation of eqn (A8) with respect to t , the following expression for the crack density dependent part $k(\rho)$ of the stress intensity factor is obtained, bearing in mind that $k(\rho, x; t)$ depend only on the ratio x/d :

$$k(\rho) = \frac{1}{\sigma} \sqrt{\frac{1}{l} \left[\frac{\partial W(t, d)}{\partial t} + \frac{2nW(t, d)}{t} \right]}. \quad (\text{A9})$$

Since the energy $W(t, d)$ is proportional to t^2 for a constant crack density, it suffices to numerically evaluate $W(t, d)$ for a unit crack length and varying crack densities.

APPENDIX B

The β^{kk} -matrices which control the release in elastic energy due to the presence of matrix cracks in the composite laminate will be derived in some detail in the present Appendix. The derivation will be performed for both interior cracks and for surface cracks. The only information necessary for the derivation is the crack dependent stress intensity factors for the types of geometries and loads under consideration. The stress intensity factors will be expressed in terms of the non-dimensional stress intensity factors introduced in eqn (24). Henceforth, a superscript (i) will indicate interior cracks and a superscript (s) will imply surface cracks. It should also be noted that the non-dimensional stress intensity factors which are essential parts of the integrands in the following integrals are not constant over the interval of integration. The dimensionless stress intensity factors depend only on the crack density, as stated previously. The crack density which the cracks actually experience during the integration, however, changes with the current crack length x as $x/d^k = x\rho^k/t^k$.

For interior cracks, as was already mentioned in Section 2.3., the only non-vanishing matrices are $\beta_{EE}^{kk(i)}$ and $\beta_{BB}^{kk(i)}$. By use of eqns (14), (24) and (25), the following integral expressions for the sought matrix components can be derived

$$\begin{aligned} \beta_{11(EE)}^{kk(i)} &= \frac{2}{(t^k)^2} \rho^k \int_0^r [k_{1(E)}^{(i)}]^2 x dx, \\ \beta_{22(EE)}^{kk(i)} &= \frac{2}{(t^k)^2} \rho^k \int_0^r [k_{2(E)}^{(i)}]^2 x dx \end{aligned} \quad (\text{B1})$$

and

$$\begin{aligned} \beta_{11(BB)}^{kk(i)} &= \frac{2}{(t^k)^2} \rho^k \int_0^r [k_{1(B)}^{(i)}]^2 x dx, \\ \beta_{22(BB)}^{kk(i)} &= \frac{2}{(t^k)^2} \rho^k \int_0^r [k_{2(B)}^{(i)}]^2 x dx. \end{aligned} \quad (\text{B2})$$

The components in eqns (B1) and (B2), except for $\beta_{11(BB)}^{kk(i)}$, are explicitly evaluated by use of the stress intensity factors from Benthem and Koiter (1972) and Tada *et al.* (1973). The stress intensity factor $K_{III(B)}$ for the linearly varying load in mode III was not found in the literature, except for vanishing crack densities. The energy associated with this type of load was therefore numerically evaluated by use of the finite element method. By application of the method described in Appendix A, the corresponding dimensionless stress intensity factor $k_{1(B)}^{(i)}$ is then readily obtained as a function of the crack density. A curve fit using the method of least squares was then utilized to obtain the following expression

Table B1. The curve fit parameters used in eqns (B3) and (B8) determining the crack density dependence of the non-dimensional stress intensity factors $k_{1(\text{B})}^{(I)}$, $k_{1(\text{B})}^{(S)}$ and $k_{2(\text{B})}^{(S)}$

j	m_j	n_j	p_j
1	10.05493	12.86057	10.12126
2	-89.57940	-112.14396	-82.06207
3	584.80881	721.76316	488.18693
4	-2447.85918	-3005.04837	-1788.094155
5	6645.60894	8184.77274	4078.46414
6	-11897.22386	-14798.87933	-5742.60137
7	13950.25741	17560.78272	4789.78918
8	-10299.98788	-13100.57208	-2141.66066
9	4339.89855	5560.03142	378.54755
10	-794.98034	-1022.56878	10.30911

$$k_{1(\text{B})}^{(I)} = \frac{\sqrt{\pi}}{2\sqrt{2}} \sum_{j=1}^{10} \frac{m_j}{2^{j-1}(1+\rho)^j} \quad (\text{B3})$$

The fitted parameters m_j are found in Table B1. The expressions in eqns (B1) and (B2) can now be explicitly evaluated, and the resulting matrix components are presented in eqns (27) and (28).

The derivation of the energy related matrices for surface cracks will be performed in accordance with the derivation above for those of interior cracks. The calculation of the energy ΔW^* according to eqn (25) requires access to the total stress intensity factors in the two present crack opening modes as functions of the current crack length, which is denoted as x . The total stress intensity factors in mode I and mode III, respectively, can be expressed in the non-dimensional stress intensity factors and the applied crack surface tractions as

$$\begin{aligned} K_{\text{I(E)}}(x) + K_{\text{I(B)}}(x) &= \tau_{2(\text{E})}^k k_{2(\text{E})}^{(S)} \sqrt{x} + \tau_{2(\text{B})}^k \left[\left(\frac{x}{t^k} - 1 \right) k_{2(\text{E})}^{(S)} + \frac{x}{t^k} k_{2(\text{B})}^{(S)} \right] \sqrt{x}, \\ K_{\text{III(E)}}(x) + K_{\text{III(B)}}(x) &= \tau_{1(\text{E})}^k k_{1(\text{E})}^{(S)} \sqrt{x} + \tau_{1(\text{B})}^k \left[\left(\frac{x}{t^k} - 1 \right) k_{1(\text{E})}^{(S)} + \frac{x}{t^k} k_{1(\text{B})}^{(S)} \right] \sqrt{x}. \end{aligned} \quad (\text{B4})$$

From a comparison between eqns (14) and (25) and using the stress intensity factors from eqn (B4), the $\beta_m^{kk(s)}$ -matrices ($m = \text{EE, EB, BE, BB}$) can now be calculated. The result is

$$\begin{aligned} \beta_{11(\text{EE})}^{kk(s)} &= \frac{2}{(t^k)^2} \gamma_1^k \int_0^{x^k} [k_{1(\text{E})}^{(S)}]^2 x \, dx, \\ \beta_{22(\text{EE})}^{kk(s)} &= \frac{2}{(t^k)^2} \gamma_2^k \int_0^{x^k} [k_{2(\text{E})}^{(S)}]^2 x \, dx, \end{aligned} \quad (\text{B5})$$

for the matrix components associated with pure extension. For the matrices which define the coupling between extension and bending, the following integrals are obtained:

$$\begin{aligned} \beta_{11(\text{EB})}^{kk(s)} &= \beta_{11(\text{BE})}^{kk(s)} = \frac{2}{(t^k)^2} \gamma_1^k \int_0^{x^k} \left[\left(\frac{x}{t^k} - 1 \right) (k_{1(\text{E})}^{(S)})^2 + \frac{x}{t^k} k_{1(\text{E})}^{(S)} k_{1(\text{B})}^{(S)} \right] x \, dx, \\ \beta_{22(\text{EB})}^{kk(s)} &= \beta_{22(\text{BE})}^{kk(s)} = \frac{2}{(t^k)^2} \gamma_2^k \int_0^{x^k} \left[\left(\frac{x}{t^k} - 1 \right) (k_{2(\text{E})}^{(S)})^2 + \frac{x}{t^k} k_{2(\text{E})}^{(S)} k_{2(\text{B})}^{(S)} \right] x \, dx. \end{aligned} \quad (\text{B6})$$

The matrix components related to pure bending have the following appearance:

$$\begin{aligned} \beta_{11(\text{BB})}^{kk(s)} &= \frac{2}{(t^k)^2} \gamma_1^k \int_0^{x^k} \left[\left(\frac{x}{t^k} - 1 \right)^2 (k_{1(\text{E})}^{(S)})^2 + \left(\frac{x}{t^k} \right)^2 (k_{1(\text{B})}^{(S)})^2 + 2 \left(\frac{x}{t^k} - 1 \right) \frac{x}{t^k} k_{1(\text{E})}^{(S)} k_{1(\text{B})}^{(S)} \right] x \, dx, \\ \beta_{22(\text{BB})}^{kk(s)} &= \frac{2}{(t^k)^2} \gamma_2^k \int_0^{x^k} \left[\left(\frac{x}{t^k} - 1 \right)^2 (k_{2(\text{E})}^{(S)})^2 + \left(\frac{x}{t^k} \right)^2 (k_{2(\text{B})}^{(S)})^2 + 2 \left(\frac{x}{t^k} - 1 \right) \frac{x}{t^k} k_{2(\text{E})}^{(S)} k_{2(\text{B})}^{(S)} \right] x \, dx. \end{aligned} \quad (\text{B7})$$

The non-dimensional stress intensity factors $k_{1(\text{E})}^{(S)}$ and $k_{2(\text{E})}^{(S)}$ can be found in the works by Benthem and Koiter (1972) and by Tada *et al.* (1973). The factors $k_{1(\text{B})}^{(S)}$ and $k_{2(\text{B})}^{(S)}$ related to the linearly varying loads could not be found in the literature, save for vanishing crack densities, for which the demanded factors are found in Tada *et al.* (1973). The crack density dependencies of $k_{1(\text{B})}^{(S)}$ and $k_{2(\text{B})}^{(S)}$ were therefore numerically evaluated by use of the

finite element method according to Appendix A. A least squares fit was then applied to achieve the resulting factors as

$$k_{1(B)}^{(s)} = \frac{4 - \pi}{\sqrt{\pi}} \sum_{i=1}^{10} \frac{n_i}{(1 + \rho)^i},$$

$$k_{2(B)}^{(s)} = 0.2455 \sqrt{\pi} \sum_{i=1}^{10} \frac{p_i}{(1 + \rho)^i}, \quad (\text{B8})$$

where the coefficients n_i and p_i are found in Table B1. From eqns (B5)–(B7), the demanded matrix components are now readily calculated and the results are presented in eqns (29)–(31).